

The neural EGF family member CALEB/NGC mediates dendritic tree and spine complexity

Nicola Brandt¹, Kristin Franke¹,
Mladen-Roko Rašin², Jan Baumgart¹,
Johannes Vogt¹, Sergey Khrulev¹,
Burkhard Hassel³, Elena E Pohl¹,
Nenad Šestan², Robert Nitsch^{1,4}
and Stefan Schumacher^{1,4,*}

¹Institute of Cell Biology and Neurobiology, Center for Anatomy, Charité—Universitätsmedizin Berlin, Berlin, Germany, ²Department of Neurobiology and Kavli Institute for Neuroscience, Yale University School of Medicine, New Haven, CT, USA and ³Institute of Cell Biochemistry and Clinical Neurobiology, University Hospital Hamburg-Eppendorf, Hamburg, Germany

The development of dendritic arborizations and spines is essential for neuronal information processing, and abnormal dendritic structures and/or alterations in spine morphology are consistent features of neurons in patients with mental retardation. We identify the neural EGF family member CALEB/NGC as a critical mediator of dendritic tree complexity and spine formation. Overexpression of CALEB/NGC enhances dendritic branching and increases the complexity of dendritic spines and filopodia. Genetic and functional inactivation of CALEB/NGC impairs dendritic arborization and spine formation. Genetic manipulations of individual neurons in an otherwise unaffected microenvironment in the intact mouse cortex by *in utero* electroporation confirm these results. The EGF-like domain of CALEB/NGC drives both dendritic branching and spine morphogenesis. The phosphatidylinositol 3-kinase (PI3K)-Akt-mammalian target of rapamycin (mTOR) signaling pathway and protein kinase C (PKC) are important for CALEB/NGC-induced stimulation of dendritic branching. In contrast, CALEB/NGC-induced spine morphogenesis is independent of PI3K but depends on PKC. Thus, our findings reveal a novel switch of specificity in signaling leading to neuronal process differentiation in consecutive developmental events.

The EMBO Journal (2007) 26, 2371–2386. doi:10.1038/sj.emboj.7601680; Published online 12 April 2007

Subject Categories: development; neuroscience

Keywords: CALEB; dendrite branching; *in utero* electroporation; PI3K-Akt-mTOR signaling; spine morphogenesis

Introduction

The development of dendritic arbors is critical to neuronal circuit formation as dendrites are the primary sites of synaptic input (Scott and Luo, 2001; Whitford *et al.*, 2002; Jan and Jan, 2003). Following dendritic tree elaboration, small protrusions called spines emerge from the dendritic shafts of many neurons. These spines are morphologically specialized, and represent the main postsynaptic compartment for excitatory input (Hering and Sheng, 2001; Yuste and Bonhoeffer, 2004). A great deal of data has been presented on the importance of transmembrane proteins for connecting extrinsic cues, which regulate spine morphogenesis, to intracellular mediators of cytoskeletal rearrangements (Ethell and Pasquale, 2005). Various steps of dendrite development have been shown to be regulated by diffusible cues such as neurotrophins (Yacoubian and Lo, 2000; Horch and Katz, 2002; Ji *et al.*, 2005), cell–cell interactions involving proteins such as Notch 1 (Šestan *et al.*, 1999; Redmond *et al.*, 2000) and β -catenin (Yu and Malenka, 2003) and neuronal activity (McAllister *et al.*, 1996; Maletic-Savatic *et al.*, 1999; Portera-Cailliau *et al.*, 2003; Tolias *et al.*, 2005). Among the proteins that transduce these signals into changes in dendritic shape are not only members of the Rho family of proteins (Govek *et al.*, 2005), but also components of some key signaling pathways. One example is the Ras-Raf-MAP kinase kinase (MEK)-mitogen-activated protein kinase (MAPK) pathway, which has been shown to be involved in activity-dependent dendrite differentiation (Wu *et al.*, 2001; Vaillant *et al.*, 2002). Another likely candidate is the phosphatidylinositol 3-kinase (PI3K)-Akt signaling pathway. This pathway has gained attention in neuroscience as it was highlighted to be implicated in neuronal growth, survival, neurite outgrowth, and synaptic plasticity (Atwal *et al.*, 2000; Kuruvilla *et al.*, 2000; Markus *et al.*, 2002; Sanna *et al.*, 2002). The PI3K has also been shown to organize dendritic branching together with Rho GTPases (Leemhuis *et al.*, 2004). One of the PI3K-Akt-regulated proteins is the protein kinase mammalian target of rapamycin (mTOR), which is thought to act primarily by regulating protein translation. PI3K-Akt-mTOR signaling not only controls synaptic plasticity (Tang *et al.*, 2002; Hou and Klann, 2004), but also dendritic arborization (Jaworski *et al.*, 2005; Kumar *et al.*, 2005).

However, the precise molecular mechanisms that transduce extracellular cues via transmembrane receptors to intracellular signaling pathways to shape dendritic arbors and spines during consecutive developmental events are not fully understood.

In this study, we characterized CALEB/NGC (Chicken Acidic Leucine-rich EGF-like domain containing Brain protein/Neuroglycan C), a member of the neural transmembrane EGF family, in the processes of dendritic tree elaboration and spine formation. CALEB/NGC is highly expressed in brain, in particular in fiber-rich areas, and the expression of this protein is upregulated during times of dendrite differentiation

*Corresponding author. Institute of Cell Biology and Neurobiology, Center for Anatomy, Charité—Universitätsmedizin Berlin, Charitéplatz 1, Berlin 10117, Germany.

Tel.: +49 30 450 528323; Fax: +49 30 450 528902;

E-mail: stefan.schumacher@charite.de

⁴These authors contributed equally to this work

(Schumacher *et al*, 1997; Aono *et al*, 2000). CALEB/NGC can bind to the extracellular matrix proteins tenascin-C and tenascin-R, and interacts with the intracellular PSD-95/Discs large/ZO-1 (PDZ) domain protein PIST (PDZ domain protein interacting specifically with TC10; Schumacher *et al*, 2001; Hassel *et al*, 2003; Schumacher and Stübe, 2003). Cell culture experiments suggested a function of CALEB/NGC in neurite formation (Schumacher *et al*, 1997; Nakanishi *et al*, 2006). Electrophysiological analysis of CALEB/NGC-deficient mice showed disturbances in maintaining normal release probability at early developmental stages (Jüttner *et al*, 2005). However, the physiological function of CALEB/NGC is still unclear. Using *in utero* electroporation, we show that CALEB/NGC stimulates dendritic tree and spine complexity in the mouse cortex *in vivo*. Further, studies in primary hippocampal neurons indicate that the enhancement of dendritic arborization by CALEB/NGC is mediated by the EGF-like domain. This effect is independent of electrical activity, but can be blocked by inhibitors of PI3K, Akt, and mTOR. It is also dependent on protein kinase C (PKC) but not on the MEK-MAPK pathway. In contrast to its effect on dendritic branching, CALEB/NGC increases the complexity of dendritic spines and filopodia independent of PI3K.

Taken together, we present novel evidence for a physiological role of CALEB/NGC in mediating dendritic tree complexity in the rodent cortex and uncover mechanisms of how CALEB/NGC drives dendritic branching and spine formation.

Results

CALEB/NGC is expressed in hippocampal and neocortical neurons and increases dendritic arborizations

In this study, we were interested in the expression of CALEB/NGC in rodent hippocampal and neocortical tissue. We found strong expression of CALEB/NGC in adult dentate gyrus (DG) and the CA1 and CA3 (Cornu Ammonis) regions, as demonstrated by indirect immunofluorescence staining with an affinity-purified polyclonal antibody to CALEB/NGC (Figure 1A1). CALEB/NGC was expressed in regions where basal or apical dendrites of pyramidal neurons elaborate (Figure 1A2). It was also expressed in postnatal day 10 (P10) mouse hippocampal tissue (Figure 1A3) and in the neocortex, in particular in the upper layers (Figure 1A4). Furthermore, CALEB/NGC was expressed in primary hippocampal neurons at 9 days *in vitro* (DIV9) and, in addition to being present in axons and cell bodies, strongly localized to dendrites (Figure 1A5–A8).

To find out whether CALEB/NGC is involved in the development of dendritic arborizations, we ectopically expressed the CALEB/NGC isoform mCALEBb or EGFP in DIV7 hippocampal neurons. After two more days in culture (DIV7 + 2), neurons were fixed and stained for mCALEBb or GFP. The dendritic trees of neurons expressing mCALEBb were much more elaborated than those of EGFP-expressing cells (Figure 1B). Compared to neurons expressing EGFP, mCALEBb-expressing cells had more complex dendritic branches, as measured by total number of dendritic end tips (TNET) of branches longer than 8 μm (Figure 1C and D; mean values and s.e.m. of all statistical calculations can be found in Supplementary Figure S6). We also coexpressed

mCALEBb together with EGFP, and compared these neurons to those that only expressed EGFP (Figure 3B). A similar increase in TNET was found (Figure 3C and D). The effects of CALEB/NGC on dendritic arbor elaboration were further analyzed using Sholl analysis, which quantifies the number of times dendrites from a neuron cross concentric circles of increasing diameter (Sholl, 1953). With this analysis, we confirmed that expression of mCALEBb enhanced dendritic tree complexity (Figure 1E).

To describe dendritic phenotypes more precisely, we determined the number of dendritic end tips of apical and basal dendrites and the number of higher order dendrites in the same experimental approach as described above. We restricted this part of analysis to those neurons with clear distinguishable basal and apical dendrites. We found that mCALEBb expression only slightly increased the number of end tips (NDET) of basal dendrites but significantly increased NDET of apical dendrites when compared to EGFP as control (Figure 1F). Expression of mCALEBb significantly increased the number of higher order dendrites (Figure 1G). Together, these results show that overexpression of CALEB/NGC increases dendritic branching of primary hippocampal neurons.

Knockdown of CALEB/NGC reduces dendritic tree complexity

To examine the impact of endogenous CALEB/NGC on dendritic tree morphogenesis, we used RNA interference with siRNA and shRNA directed to CALEB/NGC. Primary hippocampal neurons were transfected at DIV9 either with shRNA construct CAL3sh (specific for rat and mouse CALEB/NGC) or with control shRNA construct CAL1sh (derived from a part of chicken CALEB/NGC sequence, which is not conserved between chicken and rat or mouse). Three days after transfection, cells were stained for GFP (green) and CALEB/NGC (red) and analyzed. We could observe a correlation of endogenous CALEB/NGC levels and dendritic tree complexity (Figure 2B1–B5 and Supplementary Figure S1) in CAL3sh knockdown neurons. Two CAL1sh control cells are given in Figure 2A1 and A2. We determined TNET and found it to be significantly reduced in neurons targeted by CAL3sh when compared to neurons transfected with CAL1sh or pCGLH vector as control (Figure 2C). A further control of knockdown efficiency is given in Figure 2D. A Western blot was performed with detergent cell extracts of HEK293 cells co-transfected with mCALEBb and either CAL1sh or CAL3sh and stained for FLAG-tagged CALEB/NGC and β -tubulin as a loading control. We also transfected DIV10 primary hippocampal neurons with siRNA oligonucleotides CAL1 and CAL3 and analyzed the CAL3-induced reduction of endogenous CALEB/NGC by immunoblotting with a monoclonal antibody to CALEB/NGC (Figure 2E and Supplementary Figure S2). β -Tubulin was stained as a loading control. A quantitative analysis of CALEB/NGC-specific immunofluorescence signal in cell bodies of EGFP-expressing neurons corroborated the knockdown of CALEB/NGC expression by CAL3 but not by CAL1 (Figure 2F). Neurons co-transfected with CALEB/NGC-specific siRNA oligonucleotide CAL3 and EGFP-encoding plasmid had decreased CALEB/NGC expression and reduced dendritic arborization (Figure 2F and G and Supplementary Figure S3) when compared to neurons co-transfected with control oligonucleotide CAL1 and EGFP-encoding plasmid

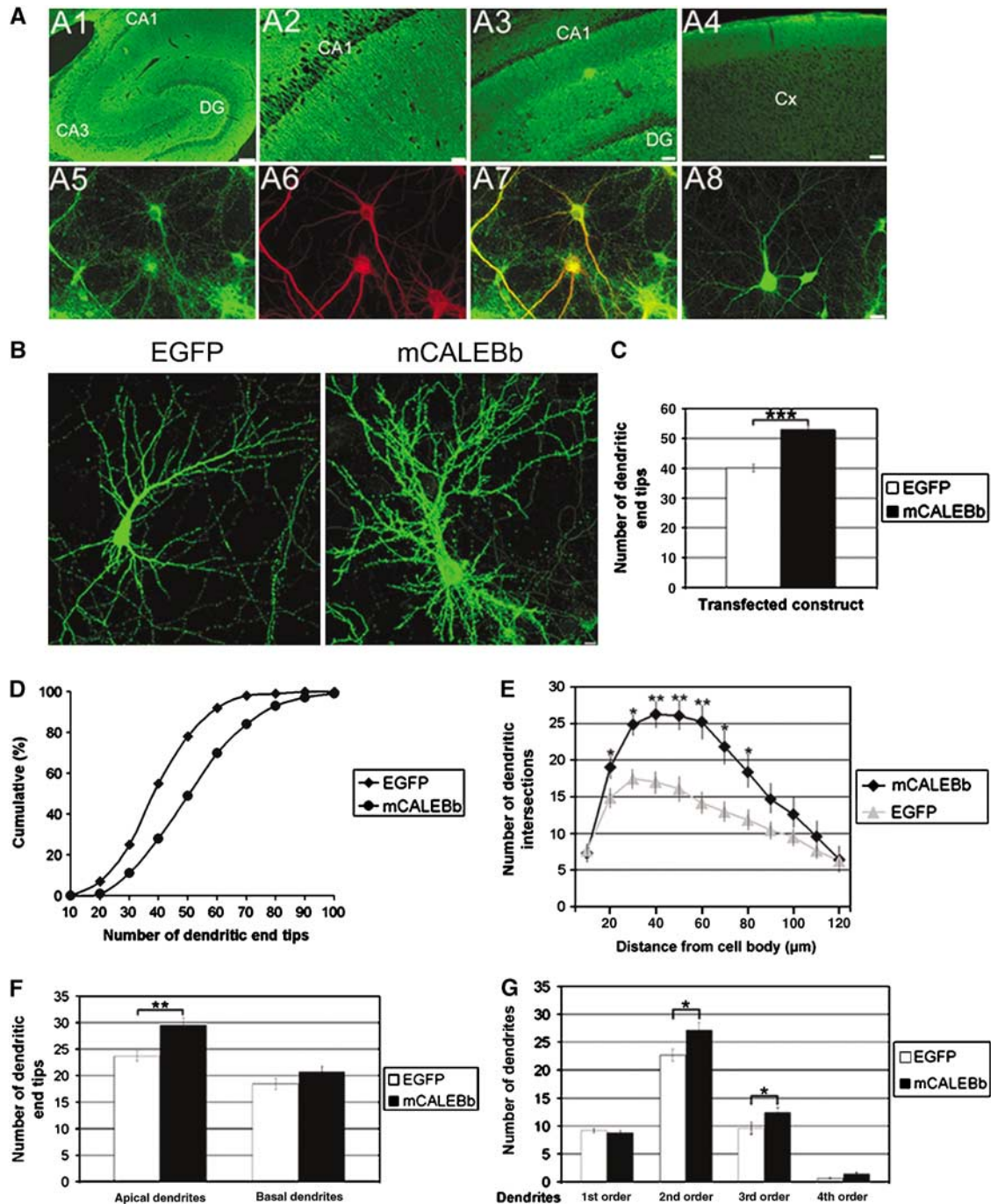


Figure 1 CALEB/NGC is expressed in hippocampal and neocortical neurons and increases dendritic arborizations. (A) A section of adult rat hippocampus was stained by indirect immunofluorescence with an antibody to CALEB/NGC (green, A1). In a high-magnification view of the CA1 region (A2) CALEB/NGC staining was found predominantly in fiber-rich areas. CALEB/NGC was also present in P10 mouse hippocampus (A3) and cortex (A4). When hippocampal cells in culture at DIV9 were probed with two different anti-CALEB/NGC antibodies (A5, A8), cell bodies and dendrites were clearly decorated. Anti-microtubule-associated protein 2 (MAP2) antibody stainings (red, A6) and overlay of anti-CALEB/NGC and MAP2 stainings (A7) confirmed dendritic localization of CALEB/NGC. (B) Examples of hippocampal neurons in culture transfected at DIV7 with either EGFP-encoding (left panel) or mCALEBb-encoding plasmid (right panel) and analyzed at DIV7+2. (C) Quantification of TNDET of hippocampal neurons transfected as described above; $n = 150$, $***P < 0.0001$. (D) Cumulative frequency plot of TNDET in neurons examined as described. (E) Neurons transfected as described above were analyzed by Sholl analysis; $n = 15$, $**P < 0.001$, $*P < 0.01$. (F, G) Effect of CALEB/NGC on total number of apical and basal dendritic branches (F) and on higher order dendritic branches (G); $n = 32$, $**P < 0.005$, $*P < 0.05$. Scale bars, 200 μm (A1), 80 μm (A2), 150 μm (A3, A4), 25 μm (A5–A8), 15 μm (B). CA, cornu ammonis; DG, dentate gyrus; Cx, cortex.

(Figure 2F and G and Supplementary Figure S3). The quantification of TNDET showed that the specific knockdown of CALEB/NGC by CAL3 resulted in a reduced number of end

tips when compared to CAL1 or EGFP alone (Figure 2G). These findings support the relevance of CALEB/NGC for regulation of dendritic arbor complexity.

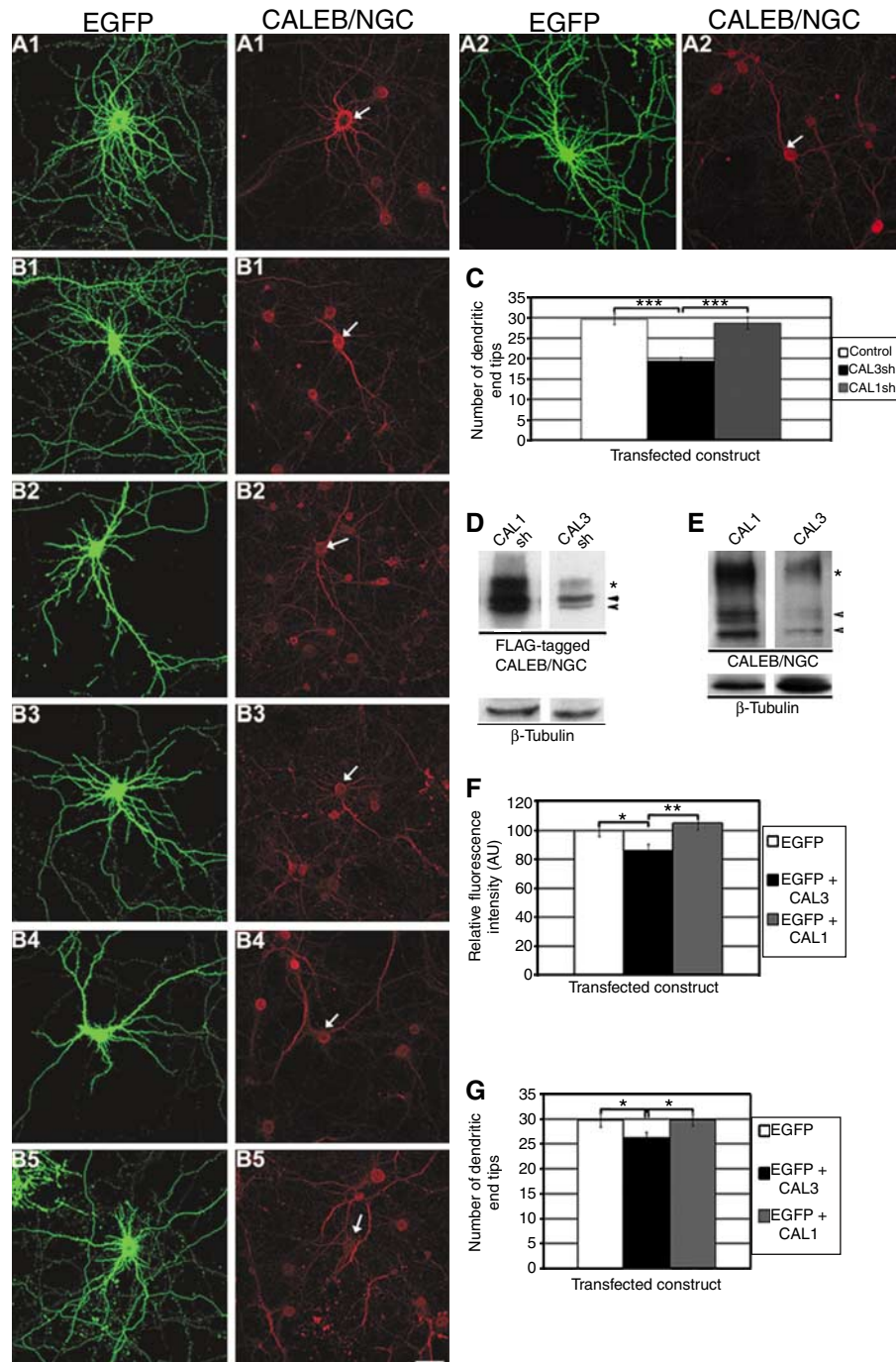


Figure 2 Knockdown of CALEB/NGC reduces dendritic tree complexity. (A, B) Hippocampal neurons in culture were transfected at DIV9 with the shRNA constructs CAL1sh (A) and CAL3sh (B) and analyzed 3 days later. A GFP staining was performed to visualize neuron morphology (A1 and A2 green, B1–B5 green). Endogenous CALEB/NGC expression was shown by staining of the culture with the anti-CSPG5 monoclonal antibody (A1 and A2 red, B1–B5 red, arrows label transfected neurons), which recognizes an epitope in the cytoplasmic domain of CALEB/NGC (see Materials and methods). (C) Quantification of TNET of hippocampal neurons transfected as described above; $n = 40$, $***P < 0.0001$. (D) Western blot of mCALEBb levels in HEK293 cells co-transfected with control shRNA construct CAL1sh or CALEB/NGC-specific shRNA construct CAL3sh and mCALEBb-encoding plasmid. The immunoblot performed 24 h after transfection was probed with either anti-FLAG antibody or anti- β -tubulin antibody (loading control). Both the mCALEBb band (doublet, arrows) and the proteoglycan variant of CALEB/NGC (*) were stained. (E) Western blot of endogenous CALEB/NGC levels in primary hippocampal neurons transfected at DIV10 with control siRNA CAL1 or CALEB/NGC-specific siRNA CAL3 and analyzed 2 days later. The immunoblot was probed with either anti-CALEB/NGC monoclonal antibody (BD Biosciences) or anti- β -tubulin antibody (loading control). Both the CALEB/NGC band (doublet, arrow) and the proteoglycan variant of CALEB/NGC (*) were stained. (F) Quantification of relative fluorescence intensities of cell bodies of hippocampal neurons transfected with the indicated siRNA constructs at DIV10 and analyzed at DIV10 + 2 after CALEB/NGC staining; $n = 30$, $*P < 0.05$ and $**P < 0.01$. AU, arbitrary units. (G) Quantification of TNET in neurons transfected as in (F); $n = 150$, $*P < 0.05$. Scale bar, 20 μ m.

The EGF-like domain and a specific cytoplasmic peptide segment of CALEB/NGC are important for increasing dendritic tree complexity

To gain insight into the intracellular regions of CALEB/NGC necessary for signal transduction to the cytoskeleton, we

transfected several CALEB/NGC-derived constructs into hippocampal neurons in culture. The cytoplasmic part of CALEB/NGC can be subdivided into four regions, A-D (Figure 3A). Construct '388', which has only cytoplasmic region A, and construct '400', that contains region B in

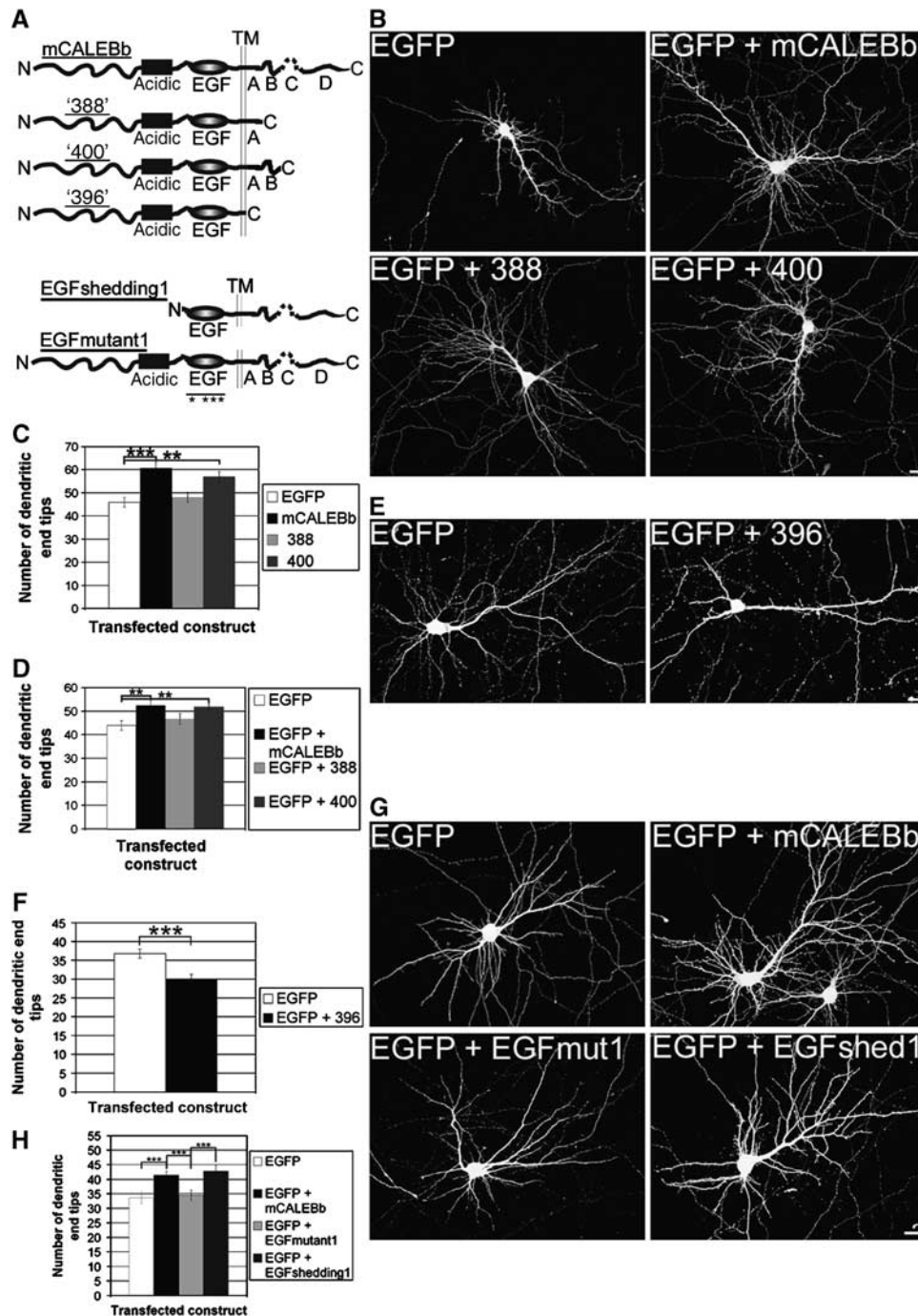


Figure 3 The EGF-like domain and a specific cytoplasmic peptide segment of CALEB/NGC are important for increasing dendritic tree complexity. (A) Scheme of transfected CALEB/NGC-derived constructs. EGF, EGF-like domain; acidic, acidic peptide segment; TM, transmembrane region. (A) Juxtamembrane cytoplasmic peptide segment of CALEB/NGC shown to bind to the PDZ protein PIST; (B) peptide segment shown to be necessary for CALEB/NGC-induced dendritic branching; (C) peptide segment generated due to alternative splicing; (D) peptide segment of unknown function. (B) Cultured hippocampal neurons were co-transfected at DIV7 with EGFP-encoding plasmid and different CALEB/NGC-derived constructs shown schematically in (A). Neurons were analyzed at DIV7+2 after staining for GFP. (C) Quantification of TNDET of transfected cells (performed as described in Figure 1; $n=42$; $***P<0.0001$ and $**P<0.005$). (D) Quantification of TNDET of neurons co-transfected as described in (B); $n=45$, $**P<0.01$. (E) Neurons were transfected at DIV12 to express EGFP or co-express EGFP and CALEB/NGC-derived construct '396', and analyzed 2 days later after staining for GFP. (F) Quantification of TNDET of neurons co-transfected as described in (B); $n=90$, $***P<0.001$. (G) Hippocampal neurons were co-transfected with the indicated constructs and analyzed as described in (B). (H) Quantification of TNDET; $n=40$, $***P<0.0001$. Scale bar, 25 μ m.

addition, were transfected into hippocampal neurons at DIV7 and analyzed at DIV7 + 2. The quantification of TNET (Figure 3C) showed that construct '400', like mCALEBb, was able to increase the complexity of dendritic arbors. To exclude the possibility that any of the CALEB/NGC-derived constructs was not correctly targeted to all dendrites, we co-transfected these constructs together with EGFP-encoding plasmid into DIV7 hippocampal cells, which were analyzed at DIV7 + 2 (Figure 3B). Quantification of TNET (Figure 3D) confirmed the result indicated above. We next analyzed the CALEB/NGC-derived construct '396', which lacks the cytoplasmic region (Figure 3A). We hypothesized that it might uncouple extracellular events (e.g. binding of a putative ligand) from intracellular signal transduction. Indeed, we found that construct '396' led to a reduction in TNET (Figure 3E and F). These findings suggest that CALEB/NGC-derived construct '396' may work in a dominant-negative manner to inhibit endogenous CALEB/NGC action.

To determine which region of the extracellular part of CALEB/NGC is necessary for promoting dendritic tree complexity, we tested several deletion constructs. We found that the construct EGFshedding1 (Figure 3A), which only contains the EGF-like domain outside the cell, was sufficient to drive dendritic branching like mCALEBb (Figure 3G). To examine whether the EGF-like domain is necessary for stimulating dendrite morphogenesis, we analyzed the construct EGFmutant1 (Figure 3A), which is identical to mCALEBb with the exception of four-point mutations in the EGF-like domain (see Materials and methods). This construct did not promote dendritic branching above EGFP control (Figure 3G). Quantification of TNET confirmed these results (Figure 3H). Thus, the EGF-like domain of CALEB/NGC drives dendritic branching.

CALEB/NGC stimulates dendritic tree complexity in mouse cortex

To explore whether CALEB/NGC is important for dendritic tree development *in vivo*, we performed analysis of mouse brain pyramidal neurons of neocortex targeted by *in utero* electroporation. This technique was chosen because it allows a selective manipulation of CALEB/NGC function in a subset of cells in otherwise normal tissue. It further allows a temporally discrete interference with endogenously expressed CALEB/NGC protein. In this way, the caveat of expression upregulation of genes that could compensate for functional loss of CALEB/NGC can be circumvented. This compensatory expression upregulation of genes might be a problem in classical genetic knockout strategies (Deuel *et al*, 2006; Koizumi *et al*, 2006).

We used the *in utero* electroporation protocol to transfect embryonic day 15.5 (E15.5) cortical neurons, mostly pyramidal neurons of cortical layers II and III *in vivo* with the constructs mCALEBb and '396' (Figure 3A) cloned into the pCLEG vector. In addition, the shRNA constructs CAL3sh and CAL1sh as control cloned into the pCGLH vector (Chen *et al*, 2005) were used. With both vectors, expression of GFP is translationally driven by an internal ribosomal entry site (IRES). Electroporated animals were examined at postnatal day 7 (P7). Examples of coronal sections of these animals stained for GFP are given in Figure 4A1–E1. In each case, cortical cells in one hemisphere were targeted. Two examples of individual pyramidal neurons for each transfection condi-

tion are presented in Figure 4A2–E3. Dendritic arbors of neurons expressing mCALEBb (Figure 4B2 and B3) were more complex, and dendritic arbors of neurons expressing construct '396' (Figure 4C2 and C3) were less complex than those of control neurons (Figure 4A2 and A3). Expression of different CALEB/NGC-derived constructs in these pyramidal neurons was shown by anti-FLAG epitope staining (Figure 4F). Analysis of mice cortices electroporated with the CAL3sh-knockdown construct specific to CALEB/NGC confirmed these results. The TNET of electroporated neurons in cortex was reduced as shown by two representative neurons (Figure 4D2 and D3) when compared to the knockdown control CAL1sh. The quantification of TNET (Figure 4G) confirmed that mCALEBb increased, constructs '396' and CAL3sh decreased dendritic tree complexity. The outcome of these experiments is that CALEB/NGC is functionally critical for establishing dendritic tree complexity of mouse pyramidal neurons *in vivo*.

The PI3K-Akt-mTOR pathway is important for CALEB/NGC-induced increase in dendritic tree complexity

To get more insight into the molecular mechanisms of CALEB/NGC function with respect to dendritic arbor elaboration, we focused on the PI3K-Akt-mTOR and the MEK-MAPK signaling pathways which have recently been shown to be important for the control of dendritic arborization (Wu *et al*, 2001; Vaillant *et al*, 2002; Jaworski *et al*, 2005; Kumar *et al*, 2005).

We used established inhibitors for specific kinases of these signaling pathways to determine the relevance of these proteins for CALEB/NGC-induced dendritic branching. Hippocampal neurons were transfected at DIV7 either with EGFP- or mCALEBb-encoding constructs, treated with these specific inhibitors and analyzed at DIV9 (Figure 5A, left and right panels, respectively). All inhibitors of the PI3K-Akt-mTOR pathway blocked CALEB/NGC-induced dendritic tree complexity, whereas U0126, a MEK inhibitor, did not (Figure 5A). In more detail, the PI3K inhibitor LY294002 fully suppressed CALEB/NGC-induced increase in TNET (Figure 5B). It also reduced dendritic branching in the control as has been published (Jaworski *et al*, 2005; Kumar *et al*, 2005).

A similar decrease in TNET was observed when applying Akt inhibitors I and III (Figure 5C). When the Akt target mTOR was inhibited by rapamycin, the CALEB/NGC-induced increase in TNET was significantly reduced (Figure 5D). However, even with two different concentrations of rapamycin, mCALEBb-transfected neurons had still more dendritic end tips than EGFP-transfected control cells. The MEK inhibitor U0126 did not lead to any inhibition of CALEB/NGC-induced increase in TNET (Figure 5E), although it was active in inhibiting the phosphorylation of MAPK (Figure 5F). Taken together, the PI3K-Akt-mTOR, but not the MEK-MAPK pathway, is important for CALEB/NGC-stimulated dendritic tree complexity.

CALEB/NGC stimulates dendritic tree complexity independent of electrical activity but dependent on PKC

A role for endogenous neuronal activity in dendritic arbor development has been highlighted (McAllister *et al*, 1996; Maletic-Savatic *et al*, 1999; Portera-Cailliau *et al*, 2003; Tolia *et al*, 2005). Ion channels that have been shown to mediate

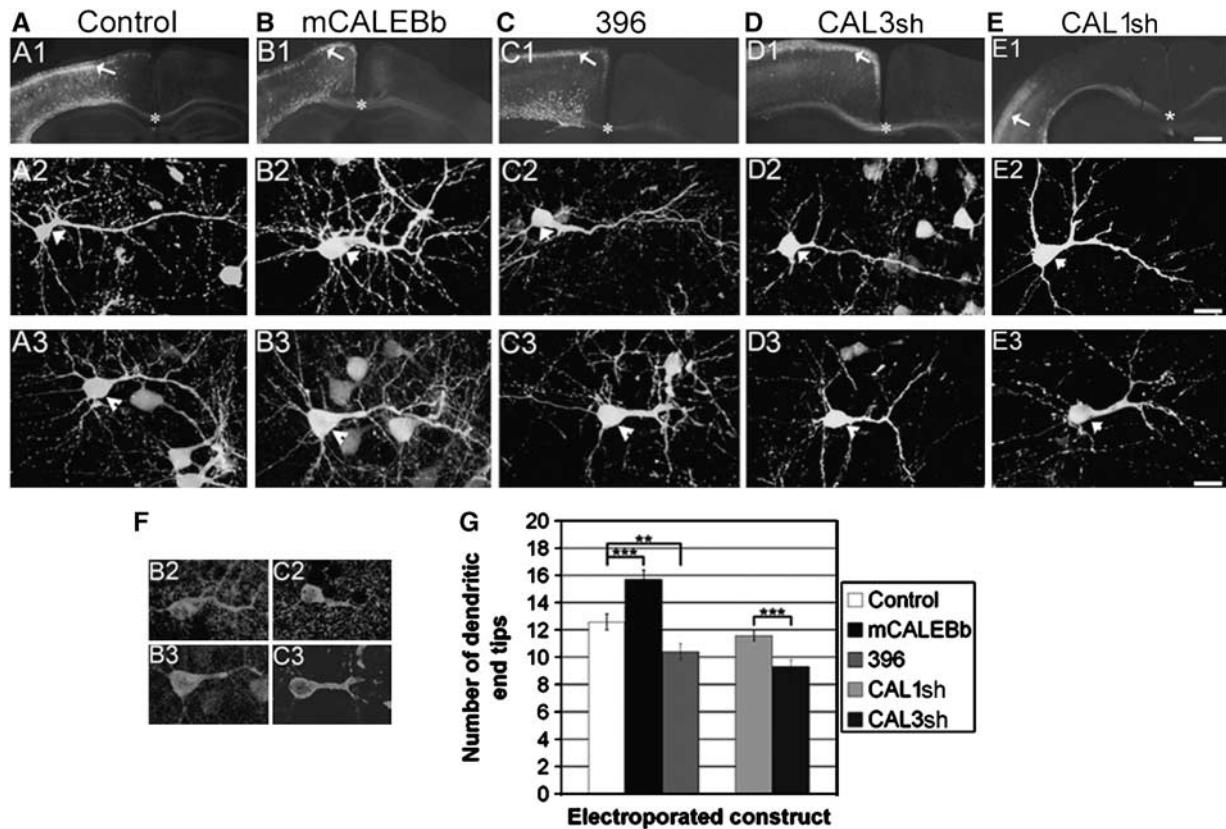


Figure 4 CALEB/NGC stimulates dendritic tree complexity in mouse cortex. (A) E15.5 mouse embryos were electroporated *in utero* with the pCLEG vector driving GFP expression. Overview of a coronal section (70 μ m thick) stained with an antibody to GFP (A1), and two examples of individual neurons of these electroporated animals (A2, A3). (B) *In utero* electroporation was performed with a construct driving mCALEBb and GFP expression. Pictures of this animal corresponding to A1–A3 are presented in B1–B3. (C) *In utero* electroporation was done with the CALEB/NGC-derived construct ‘396’ cloned into the pCLEG vector to drive expression of construct ‘396’ and GFP. Pictures of this animal corresponding to A1–A3 are presented in C1–C3. (D) The CAL3sh knockdown construct specific to CALEB/NGC cloned into the pCGLH vector that drives GFP expression was electroporated *in utero* into cortical layer II and III neurons. Pictures of this animal corresponding to A1–A3 are presented in D1–D3. (E) Pictures derived from an animal electroporated with shRNA control construct CAL1sh corresponding to A1–A3 are shown in E1–E3. (F) Expression control of mCALEBb and construct ‘396’ with an antibody to the FLAG epitope. (G) Quantification of TNET of pyramidal neurons in tissue sections of *in utero* electroporated animals. End tips of dendritic branches longer than 8 μ m were counted; $n = 40$, $**P < 0.01$, $***P < 0.001$. Arrows in A1, B1, C1, D1, and E1 indicate cortical layers 1–3; asterisks in A1, B1, C1, D1, and E1 mark the corpus callosum, arrowheads in A2–E3 point to representative neurons. Scale bars, 80 μ m (A1, B1, C1, D1, and E1), 15 μ m (A2–E3).

the effects of activity on dendritic arborization are *N*-methyl-D-aspartate receptors and L-type voltage-sensitive calcium channels (Sin *et al*, 2002; Yu and Malenka, 2003). Application of a mixture of antagonists (tetrodotoxin (TTX), D-3-amino-phosphonovaleric acid (D-APV) and nifedipine (NF)) to DIV7 hippocampal neurons decreased TNET in control conditions (Figure 6A and B). However, mCALEBb overexpression resulted in an increase in TNET even in the presence of the inhibitors TTX, D-APV, and nifedipine, when compared to EGFP-expressing cells (Figure 6A and B). These findings indicate that the effect of CALEB/NGC on dendritic tree elaboration is, at least to a large extent, independent of electrical activity.

A possible involvement of CALEB/NGC in neurite outgrowth has been published (Schumacher *et al*, 1997; Nakanishi *et al*, 2006). Data from Nakanishi *et al* (2006) suggest that the extracellular part of CALEB/NGC is able to promote neurite outgrowth via PI3K and PKC pathways. We were interested whether PKC plays a role in CALEB/NGC-stimulated dendritic branching. We found that the PKC inhibitor hypericin only very slightly affected the increase in TNET mediated by CALEB/NGC (Figure 6A and C). However, bisindolylmaleimide (BIM), another inhibitor of PKC, blocked

the increase in TNET stimulated by CALEB/NGC (Figure 6A and D). Together, these results suggest that PKC plays a role in CALEB/NGC-mediated dendrite morphogenesis.

Enhanced CALEB/NGC expression increases density and complexity of dendritic spines and filopodia

CALEB/NGC was not only expressed in main dendrites of hippocampal neurons early in development (Figure 1A), but also strongly localized to dendritic spines and filopodia during later maturation stages (Figure 7A). Therefore, the question arose whether CALEB/NGC might be involved in spinogenesis as well. To examine this, we overexpressed mCALEBb or EGFP in DIV12 hippocampal neurons in culture and analyzed spine and filopodia morphology of these cells 4 days later (DIV12 + 4). When compared with EGFP-expressing neurons (Figure 7B), the dendritic arbors of mCALEBb-expressing cells were more elaborated and contained a great many spines and filopodia (Figure 7B and C). To discriminate between spines and filopodia, we considered all dendritic protrusions $\leq 3.5 \mu$ m in length, which had a head-like structure, as spines. With this definition, we found that mCALEBb expression in hippocampal neurons induced 19% more

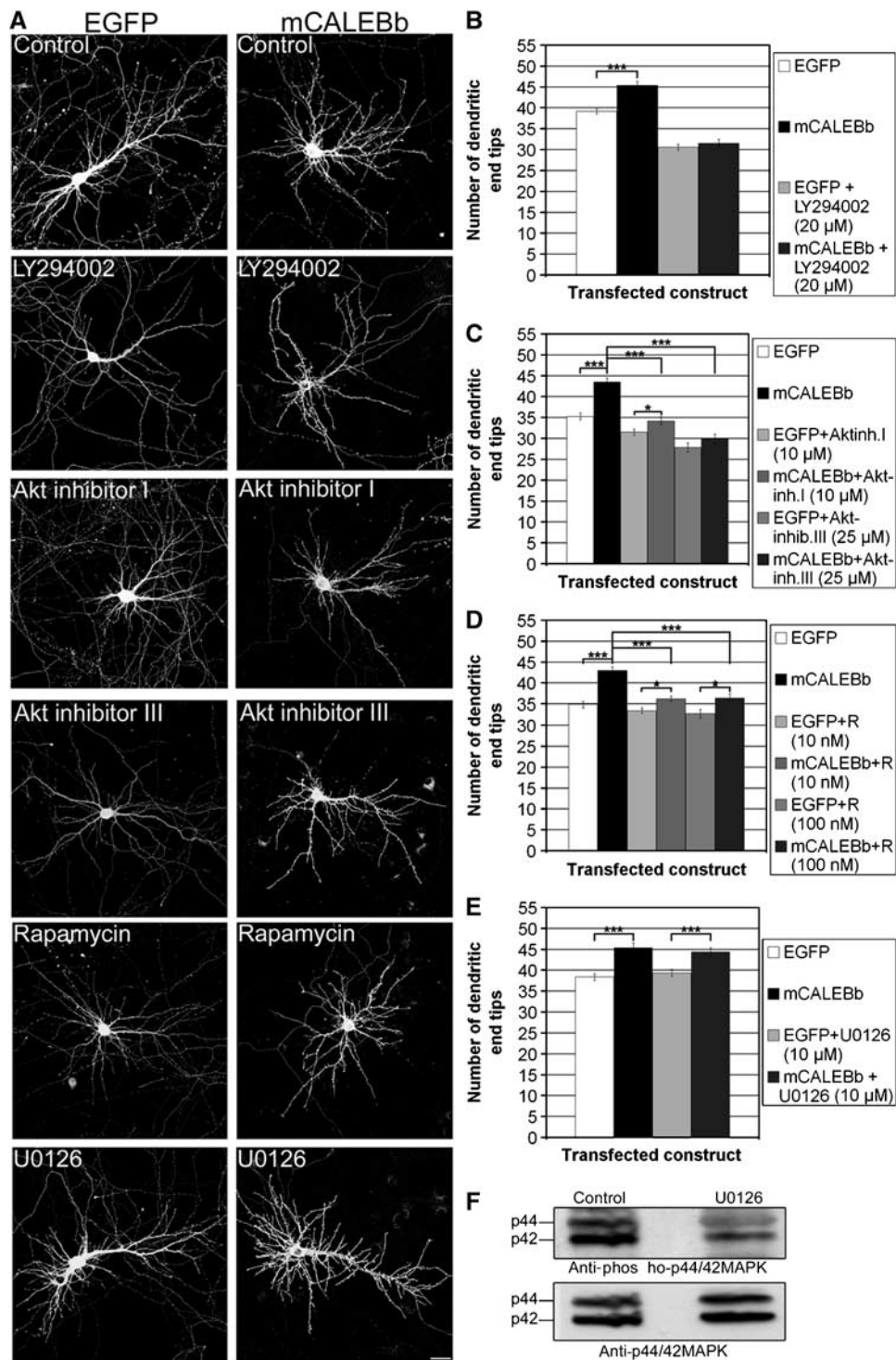


Figure 5 The PI3K-Akt-mTOR pathway is important for CALEB/NGC-induced increase in dendritic tree complexity. (A) Overall view of DIV9 hippocampal neurons transfected at DIV7 either with EGFP- (left panels) or mCALEBb-encoding plasmid (right panels) and treated with indicated concentrations of inhibitors which were added 3 h after transfection. (B) Quantification of TNET of neurons treated with or without 20 μM LY294002; $n = 81$, $***P < 0.0001$. (C) Quantification of TNET of neurons treated with or without 10 μM Akt inhibitor I or 25 μM Akt inhibitor III; $n = 87$ for Akt inhibitor I, $n = 49$ for Akt inhibitor III, $***P < 0.0001$, $*P < 0.05$. (D) Quantification of TNET of neurons treated with or without 10 or 100 nM rapamycin (R); $n = 53$, $***P < 0.0001$, $*P < 0.05$. (E) Quantification of TNET of neurons treated with or without 10 μM U0126; $n = 124$, $***P < 0.005$. (F) Western blot of detergent extracts of DIV7 hippocampal neurons treated with or without 10 μM U0126 for 2 days and stained with anti-Phospho-p44/42MAPK or anti-p44/42MAPK antibodies. Scale bar, 25 μm.

spines than EGFP expression (13% more spines if coexpressing mCALEBb with EGFP). However, one could observe that EGFP-expressing neurons developed normal spines, often with a mushroom-like shape (Figure 7C). In contrast,

mCALEBb expression resulted in longer and more irregular spines, which were frequently branched (Figure 7C). To describe the phenomena mentioned above more precisely, we quantified the length and density of spines and filopodia,

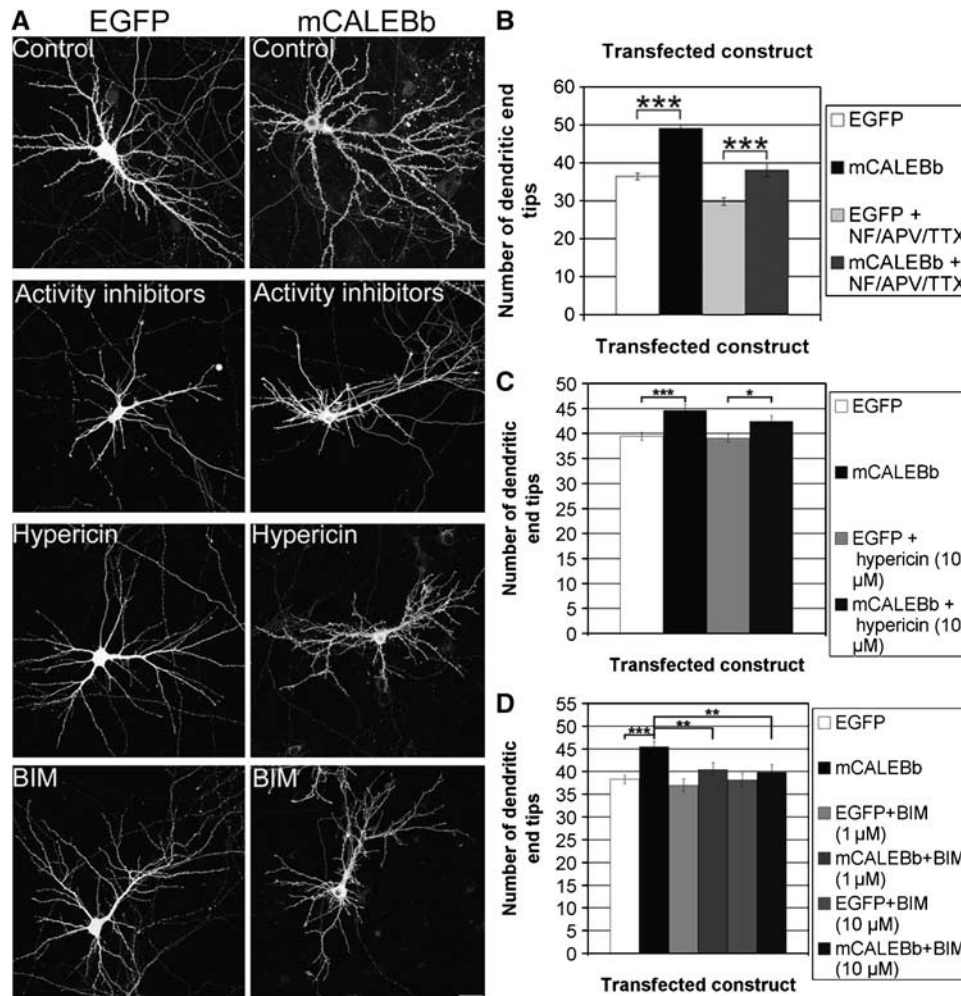


Figure 6 CALEB/NGC stimulates dendritic tree complexity independent of electrical activity but dependent on PKC. (A) Overall view of DIV9 hippocampal neurons transfected at DIV7 either with EGFP- (left panels) or mCALEBb-encoding plasmid (right panels) and treated with the indicated concentrations of inhibitors which were added 3 h after transfection. (B) Quantification of TNET of neurons treated with or without activity inhibitor cocktail (1 μM TTX, 50 μM D-APV and 10 μM nifedipine); $n = 31$ (mCALEBb + cocktail), $n = 75$ (all others), $***P < 0.0005$. (C) Quantification of TNET of neurons treated with or without 10 μM hypericin; $n = 91$, $***P < 0.0005$, $*P < 0.05$. (D) Quantification of TNET of neurons treated with or without 1 or 10 μM BIM; n (1 μM BIM) = 66, n (10 μM BIM) = 31, $***P < 0.001$, $**P < 0.01$. Scale bars, 25 μm.

as well as the density of the branch points of dendritic spines and filopodia. The expression of mCALEBb significantly increased not only the length (Figure 7D), but also the density (spines and filopodia per 10 μm) of dendritic spines and filopodia (Figure 7E). The quantification of branch-point density of dendritic spines and filopodia (branch points per 100 μm) showed that mCALEBb expression resulted in a large increase in spine and filopodia branching (Figure 7F).

To assess further the significance of CALEB/NGC for spinogenesis, we reduced the expression level of endogenous CALEB/NGC by RNA interference, and examined spine morphology. We found a smaller number of spines, which were also shorter, when compared to the control (Supplementary Figure S4).

The outcome of these experiments is that CALEB/NGC contributes to both number and morphogenesis of dendritic spines and filopodia.

CALEB/NGC increases density and complexity of dendritic spines and filopodia in mouse cortex

To examine whether CALEB/NGC is involved in spine formation in the intact brain, we performed *in utero* electro-

poration of E14.5 mouse embryos with the same constructs as described in Figure 4. At P14, we analyzed spine morphology of the electroporated animals by staining brain sections for GFP. We determined spine length, density, and branch density for each electroporated construct. Spine and filopodia length was significantly increased by construct mCALEBb, and significantly reduced by construct '396' and CAL3sh when compared to controls (Figure 8A and B), as was spine and filopodia density (number per 10 μm; Figure 8C). CALEB/NGC also increased branching of spines and filopodia as measured by branch-point density of spines and filopodia per 100 μm (Figure 8D). These results indicate an involvement of CALEB/NGC in spine morphogenesis in the intact brain.

The EGF-like domain of CALEB/NGC drives spine and filopodia morphogenesis independent of PI3K but dependent on PKC

We showed that the EGF-like domain of CALEB/NGC is important for stimulating dendritic arbor complexity. Does this domain also contribute to spine morphogenesis? To examine this, we analyzed spine and filopodia morphology

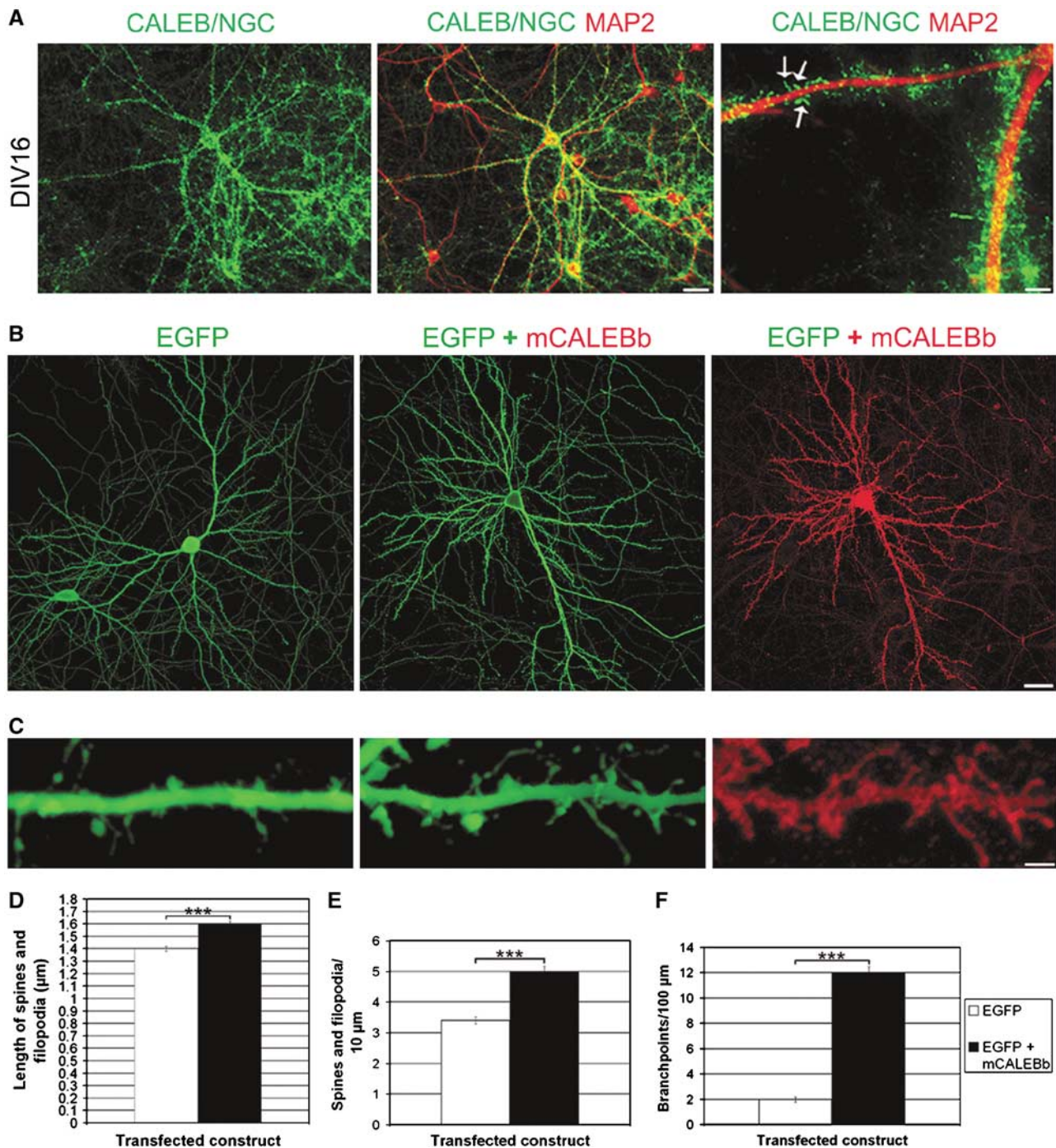


Figure 7 Enhanced CALEB/NGC expression increases density and complexity of dendritic spines and filopodia. (A) Probing hippocampal cells in culture at DIV16 with an antibody to CALEB/NGC demonstrated strong expression in dendritic processes (green, left panel). A higher magnification view (right panel) of an overlay of CALEB/NGC (green) and MAP2 staining (red, middle and right panels) showed CALEB/NGC to be located in both dendritic spines and filopodia (arrows). (B, C) Hippocampal cells in culture were either transfected at DIV12 with EGFP- (left panels in B and C) or co-transfected with EGFP- and mCALEBb-encoding plasmids (middle and right panels in B and C), and examined at DIV12 + 4 after staining for GFP (left and middle panels in B and C) or CALEB/NGC (right panels in B and C). (D) Quantification of spine and filopodia length in neurons transfected as described above; 1080 spines and filopodia $\leq 4.5 \mu\text{m}$ of 14 neurons examined for each construct; $***P < 0.0001$. (E) Quantification of spine and filopodia density (number per $10 \mu\text{m}$); 1080 spines and filopodia $\leq 4.5 \mu\text{m}$ of 14 neurons examined for each construct; $***P < 0.0001$. (F) Quantification of spine and filopodia branch density (number of branch points per $100 \mu\text{m}$; branch points of spines and filopodia $\leq 4.5 \mu\text{m}$ of $2700 \mu\text{m}$ dendrite length of 14 neurons were counted; $***P < 0.0001$. Scale bars, $35 \mu\text{m}$ (A, left and middle panel), and $6 \mu\text{m}$ (A, right panel), $25 \mu\text{m}$ (B), and $1.5 \mu\text{m}$ (C).

of DIV16 hippocampal neurons co-transfected with the constructs indicated in Figure 9A, in comparison to EGFP-expressing cells. We found that construct EGFshedding1 (Figure 3A) induced a similar phenotype in spine and

filopodia morphology as mCALEBb. In contrast, neurons expressing EGFmutant1 had a similar spine phenotype as neurons expressing EGFP (Figure 9A). EGFshedding1 expression increased mean spine and filopodia length, EGFmutant1

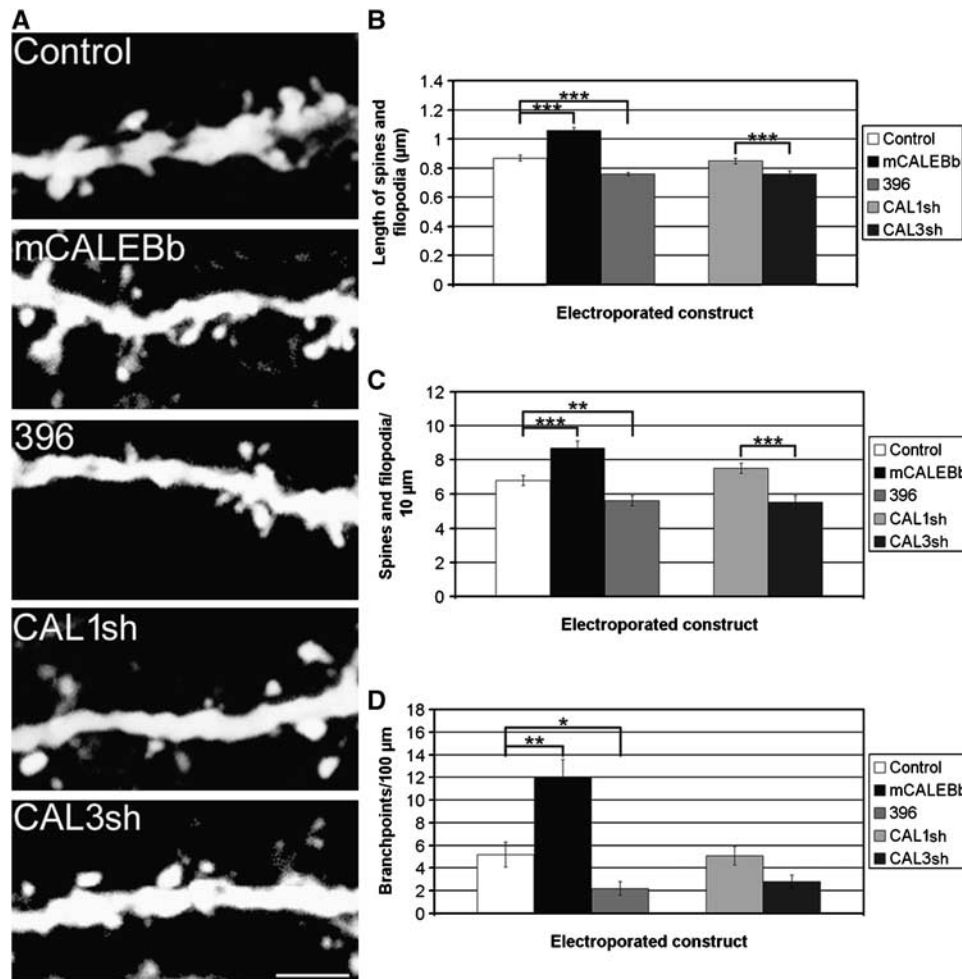


Figure 8 CALEB/NGC increases density and complexity of dendritic spines and filopodia in mouse cortex. (A) E14.5 mouse embryos were electroporated in utero with pCLEG vector (control) and the indicated constructs. Brain sections of electroporated animals were analyzed after fixation at postnatal day 14 (P14) and staining for GFP for better visualization of spine and filopodia morphology. Representative micrographs of dendritic spines and filopodia are given for each electroporated construct. (B) Quantification of spine and filopodia length in neurons electroporated as described above; 500 (for constructs mCALEBb, CAL1sh, and CAL3sh) and 660 (for pCLEG vector and construct '396') spines and filopodia $\leq 4.5 \mu\text{m}$ of 12 neurons were examined for each construct; $***P < 0.0005$. (C) Quantification of spine and filopodia density; 650 spines and filopodia of 12 neurons were counted for each construct, $***P < 0.001$, $**P < 0.01$. (D) Quantification of spine and filopodia branch density; 650 spines and filopodia of 12 neurons were analyzed, $**P < 0.01$, $*P < 0.05$. Scale bar, $2.5 \mu\text{m}$.

did not (Figure 9B). In addition, EGFshedding1 expression increased mean spine and filopodia density (number of spines and filopodia per $10 \mu\text{m}$ dendrite), whereas construct EGFmutant1 did not (Figure 9C). Furthermore, the mean branch-point density of spines and filopodia (branch points per $100 \mu\text{m}$ dendrite) was increased by construct EGFshedding1 but not by construct EGFmutant1 (Figure 9D). Thus, the EGF-like domain of CALEB/NGC is relevant for spine morphogenesis.

Is it possible that not only the same extracellular domain, but also the same signal transduction pathway plays a role for CALEB/NGC to stimulate spine morphogenesis as well as dendritic branching? To answer this question, we analyzed the effect of the PI3K inhibitor LY294002 on CALEB/NGC-induced increase in spine and filopodia length. We found that LY294002 did not inhibit the effect of CALEB/NGC on spine and filopodia length (Figure 9F). To confirm these results, we analyzed neurons transfected to express either mCALEBb alone or EGFP. In this case, the expression of mCALEBb in individual neurons was higher than in neurons co-transfected with EGFP (because of promoter competition), as was the

effect on spine and filopodia length (Figure 9G). In this situation, also LY294002 did not inhibit the increase in spine and filopodia length evoked by CALEB/NGC (Figure 9G).

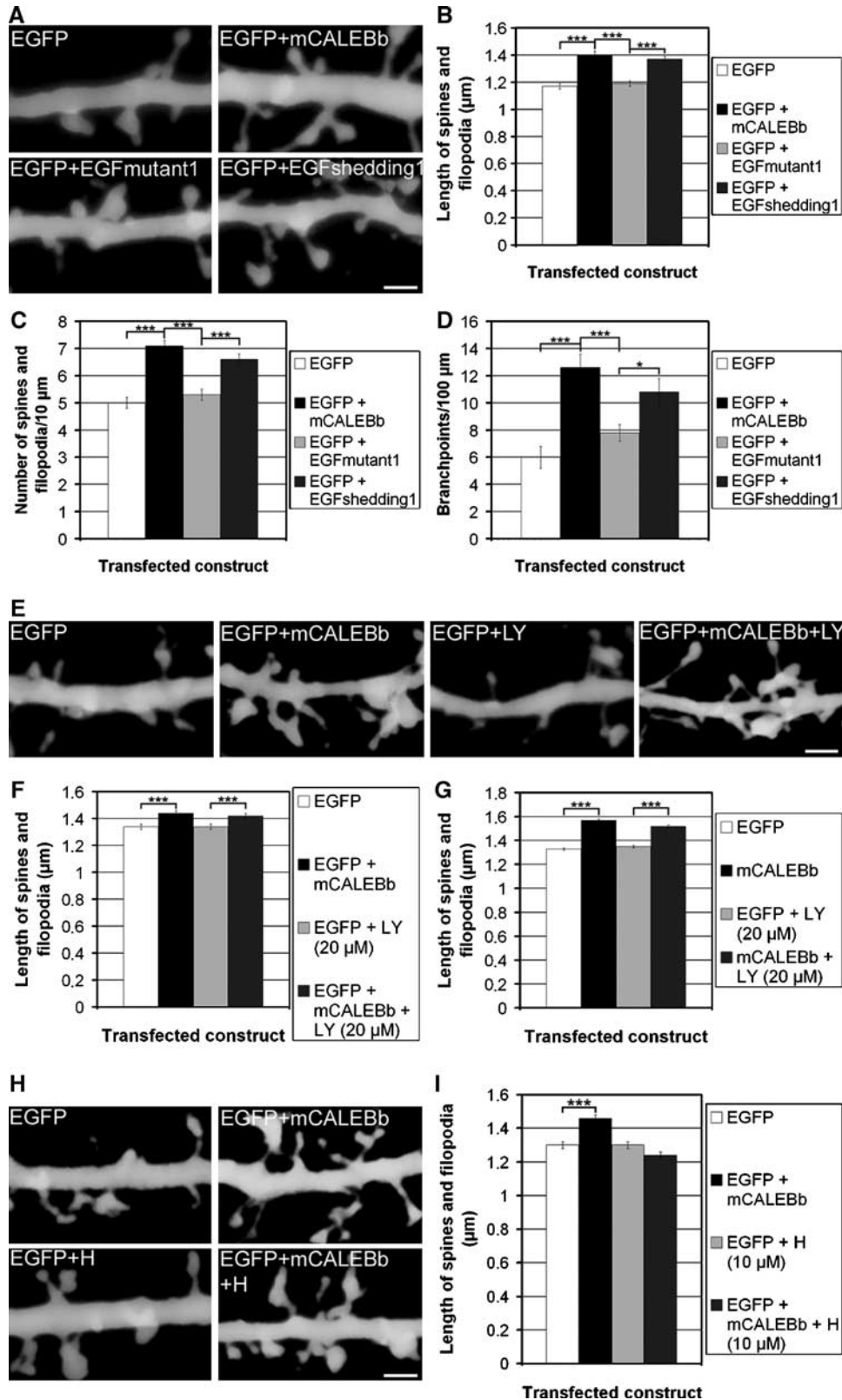
Although PI3K is important for dendritic branching stimulated by CALEB/NGC, it is not relevant for the signal transduction initiated by CALEB/NGC to drive spine morphogenesis. What about PKC, which was also shown to be necessary for dendritic branching stimulated by CALEB/NGC? We found that the PKC inhibitor hypericin, which was better tolerated by hippocampal neurons in this age (DIV12–DIV16) than BIM, could block CALEB/NGC-induced increase in spine and filopodia length (Figure 9H and I). Together, our data indicate that PKC is an important component for the signaling pathway involved in CALEB/NGC-driven spine morphogenesis.

Discussion

Dendrite morphogenesis has an important impact on neuronal circuit formation, and the extent of the arborization of

dendritic trees correlates with the number and distribution of synaptic inputs that neurons can receive and process. Here, we present data showing that CALEB/NGC mediates dendritic tree complexity and is critically involved in spine formation.

Increasing CALEB/NGC levels in primary hippocampal neurons is sufficient to enhance dendritic arborization in these cells. In fact, CALEB/NGC is strongly expressed in hippocampal and neocortical neurons during development and in the adult, and it is present in areas where basal or



apical dendrites elaborate. In hippocampal neurons in culture, a well-established model system for studying dendrite differentiation, CALEB/NGC localized to dendrites early in development and to dendritic spines and filopodia during later developmental stages. Overexpression of CALEB/NGC results in increased dendritic arbor complexity due to enhanced dendritic branching, as shown by Sholl analysis. Reducing the endogenous expression level of CALEB/NGC impairs dendritic tree elaboration. In addition, the CALEB/NGC-derived construct '396' interferes in a dominant-negative manner with endogenous CALEB/NGC function. One possible explanation for this is that construct '396' is able to bind and take away an unknown CALEB/NGC ligand but is unable to stimulate signal transduction to the cytoskeleton, because it lacks cytoplasmic peptide segments A and B. These segments are shown to be necessary for CALEB/NGC to induce dendritic arbor complexity. It will be important in future to identify interaction partners for these peptide segments which could connect the transmembrane protein CALEB/NGC to intracellular signaling pathways which, in the end, lead to increased dendritic arbor complexity. Our data show that the PI3K-Akt-mTOR pathway plays an important role in CALEB/NGC-mediated dendritic branching as pharmacological intervention at different steps of this pathway partially or fully inhibits the effects on dendritic tree complexity evoked by CALEB/NGC. The general relevance of the PI3K-Akt-mTOR pathway for dendritic branching has been published recently (Jaworski *et al*, 2005; Kumar *et al*, 2005). However, there must be several specific aspects within this pathway in terms of a fine-tuning necessary to establish a special phenotype of dendritic arbor complexity. For example, Jaworski *et al* (2005) published that basal dendrites are affected by inhibiting mTOR with rapamycin or anti-mTOR shRNA. We show that CALEB/NGC primarily stimulates branching of apical dendrites. Kumar *et al* (2005) presented data that constitutive active PI3K or Akt increase the number of first-order dendrites. Our results point to the view that CALEB/NGC affects higher order dendritic branching. One could speculate whether other signal-transducing proteins such as PKC, which is also necessary for CALEB/NGC-mediated dendritic arborization, are involved in this fine-tuning of dendritic branching.

What is the exact mechanism how CALEB/NGC acts? We favor a model in which overexpressed CALEB/NGC functions as a receptor for a so far unknown ligand and turns on its normal signal-transduction pathway. Alternatively, overexpressed CALEB/NGC could act in a dominant-negative manner by competing with endogenously expressed CALEB/NGC for cytoplasmic signaling proteins. Owing to overexpression,

many CALEB/NGC molecules would not get a ligand because the presumed ligand may not be similarly upregulated in the culture, and thus cannot drive signal transduction. However, in this scenario construct '396' must evoke the same phenotype as mCALEBb, because it competes with endogenously expressed CALEB/NGC for the presumed ligand. The construct '396'-induced dendritic phenotype, however, is very different from the mCALEBb-induced one. In addition, we observe that mCALEBb overexpression stimulates dendritic tree complexity better in dense cultures than in thin ones. We interpret this phenomenon such that mCALEBb functions as a receptor that needs a ligand produced by the culture. Which part of CALEB/NGC binds to this ligand? Our mapping experiments clearly demonstrate that the EGF-like domain of CALEB/NGC is necessary for increasing dendritic branching. A putative ligand for this domain is currently unknown. It was published that CALEB/NGC might bind to ErbB3 receptor tyrosine kinase (Kinugasa *et al*, 2004). However, the expression profile of ErbB3 does not support a relevance of ErbB3 for CALEB/NGC-induced dendritic branching (Fox and Kornblum, 2005).

A shedding of extracellular segments of CALEB/NGC, which is induced by electrical activity, has been reported (Jüttner *et al*, 2005). We show that CALEB/NGC stimulates dendritic tree elaboration independent of electrical activity. This result is in line with our data that show that the MEK inhibitor U0126 does not block CALEB/NGC-mediated dendritic branching, because the MEK-MAPK pathway has been shown to be involved in activity-dependent formation of dendrites. This either implies that the shedding of CALEB/NGC induced by electrical activity is not necessary for CALEB/NGC to increase dendritic arbor complexity, but may serve other functions. Alternatively, it could be that a shedding of extracellular segments of CALEB/NGC to expose the EGF-like domain may be stimulated by other signaling pathways.

In addition to stimulating dendritic branching, CALEB/NGC promotes spine morphogenesis by increasing their number and length. Interestingly, CALEB/NGC also promotes the branching of these dendritic protrusions. This could result in the formation of additional postsynaptic sites for the same axonal terminal. Although the EGF-like domain of CALEB/NGC drives both, dendritic branching and spine morphogenesis, different signal transduction pathways seem to be important for these effects to occur during consecutive developmental events. In case of dendritic branching, the PI3K-Akt-mTOR pathway and PKC are important, whereas in case of spine morphogenesis, PI3K is dispensable.

Figure 9 The EGF-like domain of CALEB/NGC drives spine and filopodia morphogenesis independent of PI3K but dependent on PKC. (A) DIV12 hippocampal neurons were co-transfected with the indicated constructs (Figure 3A) and spine morphology was analyzed 3 days later after staining for GFP (co-staining for GFP and FLAG epitope in case of CALEB/NGC-derived constructs). Representative micrographs of dendritic spines and filopodia are given for each transfected construct. (B–D) Quantifications of spine and filopodia length, density and branch density of neurons transfected as described in (A); 1000 spines and filopodia $\leq 4.5 \mu\text{m}$ of 12 neurons were analyzed for each construct, $***P < 0.0005$, $*P < 0.05$. (E) Representative pictures of spines and filopodia of hippocampal neurons co-transfected at DIV12 with the indicated constructs and treated for 3 days with $20 \mu\text{M}$ LY294002, which were added 3 h after transfection. (F) Quantification of spine and filopodia length of neurons transfected as described in (E); 719 (without inhibitor) and 1265 (with inhibitor) spines and filopodia $\leq 4.5 \mu\text{m}$ of 12 neurons were analyzed for each construct, $***P < 0.0005$. (G) Quantification of spine and filopodia length of neurons transfected with constructs encoding EGFP or mCALEBb at DIV12, treated with LY294002 as described above and examined 3 days later after staining for GFP or FLAG epitope; 3000 spines and filopodia $\leq 4.5 \mu\text{m}$ of 36 neurons were analyzed for each construct, $***P < 0.001$. (H) Representative pictures of spines and filopodia of hippocampal neurons co-transfected at DIV12 with the indicated constructs and treated for 3 days with $10 \mu\text{M}$ hypericin which were added 3 h after transfection. (I) Quantification of spine and filopodia length of neurons transfected as described in (H); 1350 spines and filopodia $\leq 4.5 \mu\text{m}$ of 12 neurons were analyzed for each construct, $***P < 0.0001$. Scale bar, $1.5 \mu\text{m}$.

Our data obtained from primary hippocampal neurons point to a function of CALEB on the dendritic and postsynaptic side. Recently, Rathjen and colleagues published a phenotype analysis of CALEB/NGC-deficient mice (Jüttner *et al*, 2005). They focused on electrophysiological measurements in the superior colliculus. Their results suggest that CALEB/NGC may be implicated in the development of the presynapse by affecting the release probability during early postnatal stages. Therefore, the use of this deficient mouse model for studies on the involvement of CALEB in dendritic maturation *in vivo* cannot exclude a potential presynaptic cause of postsynaptic dendritic changes. To circumvent this restriction of a CALEB/NGC-deficient mouse model for our *in vivo* studies, we took advantage of the *in utero* electroporation technique to study the function of CALEB/NGC in mouse cortex. In contrast to the situation of a knockout mouse or overexpressing transgenic animal, this technique enables studies on a small number of identifiable, genetically targeted neurons in an otherwise unaffected microenvironment. In this way, we were able to assess the selective effect of CALEB/NGC on the dendritic or postsynaptic compartment.

We electroporated CALEB/NGC-derived constructs at E14.5 (for analysis at P14) or E15.5 (for analysis at P7) to perform a temporally discrete interference with the function of endogenously expressed CALEB/NGC. We slightly overexpressed mCALEBb or misexpressed construct '396', which interferes with CALEB/NGC function in a dominant-negative manner. In addition, we reduced the amount of endogenously expressed CALEB/NGC by the shRNA construct CAL3sh. All constructs functioned *in vivo* as they did *in vitro*: mCALEBb increased, and constructs '396' and CAL3sh decreased dendritic tree complexity and spine morphogenesis. Because the number of primary dendrites starting to grow from the cell bodies only slightly increased in the case of mCALEBb electroporation compared to control (no change in the case of construct '396' and CAL3sh electroporation compared to control, data not shown), CALEB/NGC seems to operate by stimulating dendritic branching, as is also indicated by the results of the Sholl analysis (Figure 1E).

Could the electrophysiological phenotype of CALEB/NGC-deficient mice be explained by the morphological phenotype induced by CALEB/NGC in our experimental systems? This seems to be difficult. First, our *in vivo* experiments are designed to study a phenotype related directly to changes on the dendritic and not axonal site. Jüttner *et al* (2005) postulated an effect of CALEB/NGC on the presynaptic site. Second, the electrophysiological phenotype in CALEB/NGC-deficient mice can be observed only during early developmental stages (P1–P3). Our spine analysis *in vivo* shows that CALEB/NGC is involved in spine morphogenesis later in development at P14. This does not relate to the lack of electrophysiological phenotype in CALEB/NGC-deficient mice at this developmental stage. However, it would be interesting perspective to characterize electrophysiologically pyramidal neurons ectopically targeted by *in utero* electroporation with CALEB/NGC-derived constructs to better understand this issue. It is also possible to think about an axonal phenotype induced by CALEB/NGC in addition to the dendritic one which is described here, because CALEB/NGC is also expressed on axons in addition to dendrites (Schumacher *et al*, 1997). It is currently not clear whether CALEB/NGC affects only dendrites and not axons as was

published for the Ig family protein Dasm1 (Shi *et al*, 2004b), which induces a dendritic phenotype similar to CALEB/NGC. Whether CALEB/NGC functionally resembles Dasm1 in controlling excitatory synapse formation at later developmental stages (Shi *et al*, 2004a) remains to be examined in future.

In summary, we have presented *in vitro* and *in vivo* evidence that CALEB/NGC is critical for the regulation of key steps involved in generating dendritic tree complexity and spine formation.

Materials and methods

Cell culture and transfection

Primary hippocampal neurons were prepared from embryonic day 18–19 Wistar rat pups as described (Banker and Goslin, 1998). The cells were cultured on poly-L-lysine-coated glass coverslips in neurobasal A medium supplemented with 2% B27 (Invitrogen), 0.5 mM glutamine (Brewer *et al*, 1993), and the antibiotics penicillin and streptomycin at a density of 150 000 cells/well. No glia co-cultures were used.

These cells were transfected with Effectene (Qiagen) according to the manufacturer's instructions.

The ratio of EGFP and CALEB/NGC construct transfection efficiency is approximately 5:1. As indicated, an inhibitor cocktail containing TTX (1 μ M), D-APV (50 μ M) and nifedipine (10 μ M) (all from Sigma) as well as LY294002 (20 μ M), U0126 (10 μ M), hypericin (10 μ M) (all from Sigma), Akt I (10 μ M) and Akt III inhibitor (25 μ M), rapamycin (10, 100 nM) and BIM (1, 10 μ M) (all from Calbiochem) were added to the cultures 3 h after transfection. In control cultures, the equivalent volume of solvent for inhibitors was added.

Constructs and siRNA

The construct mCALEBb represents full-length CALEBb/NGC (Schumacher *et al*, 2001), with an N-terminal 3 \times FLAG tag and a C-terminal Myc epitope, cloned into the expression vector p3 \times FLAG-Myc-CMV-25 (Sigma). Construct '388' is similar to mCALEBb but lacks the part of the sequence starting from amino acids 'NKFRTPE' to the C terminus. Construct '400' is similar to mCALEBb, but lacks the part of sequence starting from amino acids 'VRKFCDDTP' to the C terminus. Construct '396' contains the whole extracellular part and the transmembrane segment of mCALEB but lacks the entire cytoplasmic region. Construct EGFshedding1 is a deletion construct of mCALEBb starting from amino acids 'VPPQHLL' to the C terminus. Construct EGFmutant1 is identical to mCALEBb but has a four-point mutation within the EGF-like domain. The sequence encoding the mutated EGF-like domain in this construct is as follows: (5'-TGTGACCTCTTTCCGAGTTACTGT-CACAACGGCGACCAGTGCTACCTGTTGGAGAACATAGGGGCTTTCTGCAGGTGTAACACCCAGGACTACATCTGGACAAGGAGATGGGCGGTGAGTCCATCATCAG-3'). The synthesized (Dharmacon) siRNA oligonucleotide CAL3 (5'-AAGCUGAGGAGGACCAACAA-A-3') for rat and (5'-AAGCUGCGGAGGACCAATAA-A-3') for mouse was derived from the rat or mouse CALEB/NGC sequence, the control siRNA oligonucleotide CAL1 (5'-AACCCCAACCCAGCCUUGAU-3') from that part of the chicken CALEB/NGC sequence not conserved between chick and rat (Schumacher *et al*, 2001). Sequence specificity of the oligonucleotides was confirmed by GenBank analysis. siRNAs were either transfected alone (400 pmol per six-well for Western blot analysis) or co-transfected with EGFP (80 pmol per 12-well) according to the Effectene transfection protocol provided by the manufacturer. Transfection efficiency is much better when transfecting only siRNA oligonucleotides than co-transfecting siRNA and EGFP. We obtained approximately 70–85% transfection efficiency with siRNA oligonucleotides (some authors report about transfection efficiencies of primary neurons up to 90% for siRNA duplexes (Govek *et al*, 2004)).

ShRNAs were constructed with the pCGLH vector (Chen *et al*, 2005) and the corresponding CAL3 and CAL1 oligonucleotides according to Brummelkamp *et al* (2002). The sequence for the hairpin is 5'-GATCTCG X TTCAAGAGA Y TTTTGTGGAAC-3', and 5'-TCGAGTTCCAAAAA X TCTCTTGAA Y CGA-3'. X, RNAi oligos; Y, complement sequence of RNAi oligos.

All constructs were tested by DNA sequencing.

Biochemical procedures

Hippocampal cell extracts were prepared with Tris-buffered saline (pH 7.4), containing 1.2% Triton X-100 and a protease inhibitor cocktail containing leupeptin, pepstatin, aprotinin, and PMSF (all from FLUKA). Protein concentrations were determined with the BCA micro protein assay (Pierce). After performing an SDS-PAGE with 8% acrylamide under reducing conditions, a subsequent Western blot was analyzed with a monoclonal antibody to CALEB/NGC (BD Biosciences, # 610986) and a polyclonal antibody to β -tubulin (H-235, Santa Cruz). Proteins were detected using a chemiluminescent detection system (LumiGLO™ Reagent and Peroxide; Cell Signaling Technology).

In utero electroporation

A detailed protocol for in utero electroporation (Saito and Nakatsuji, 2001) and selection of pyramidal neurons is presented in Supplementary Figure S5.

Immunohistochemistry and immunocytochemistry

For immunohistochemical analysis of hippocampal tissue, adult rats or P10 mice were deeply anesthetized and killed by transcardial perfusion with 4% paraformaldehyde. Cryostat sections (16 μ m thick) were prepared and after permeabilization in PBS supplemented with 5% fetal calf serum and 0.2% Triton X-100, incubated with an affinity-purified polyclonal antibody to the extracellular part of CALEB/NGC (1 μ g/ml in PBS supplemented with 5% fetal calf serum). Alexa Fluor 488-conjugated goat anti-rabbit secondary antibody (Molecular Probes) was used. Hippocampal cells in culture were indirectly stained after permeabilization with polyclonal antibodies directed to either the extracellular or the intracellular region of CALEB/NGC (both 1 μ g/ml; both directed to recombinant fusion proteins with maltose binding protein or glutathione S-transferase, respectively). Cells were co-stained with

a monoclonal antibody to MAP2 (HM-2, Sigma). The secondary antibodies Alexa Fluor 488-conjugated goat anti-rabbit (Molecular Probes) and Cy3-conjugated goat anti-mouse (Dianova) were used according to the manufacturer's instructions. Cells were imaged with a fluorescence microscope (Olympus, BX 50) equipped with a Cool SNAP ES digital camera (Roper Scientific). For fluorescence imaging, the filters U-MWIG, U-MNIBA, and U-MWU2 (Olympus) were used. For higher magnification pictures, an oil immersion objective (PLAN APO \times 60, 1.4 NA) was used.

Image acquisition and data analysis

Acquisition and data analysis for all experiments were performed by investigators blind to the experimental conditions.

A detailed description for image acquisition and data analysis is presented in Supplementary Figure S5.

Statistical analysis

Measured data were exported to Excel software (Microsoft). All results are reported as mean \pm standard error of the mean (s.e.m.). Comparison of data and calculation of *P* values were carried out using two-tailed Student's *t*-tests.

Supplementary data

Supplementary data are available at *The EMBO Journal* Online (<http://www.embojournal.org>).

Acknowledgements

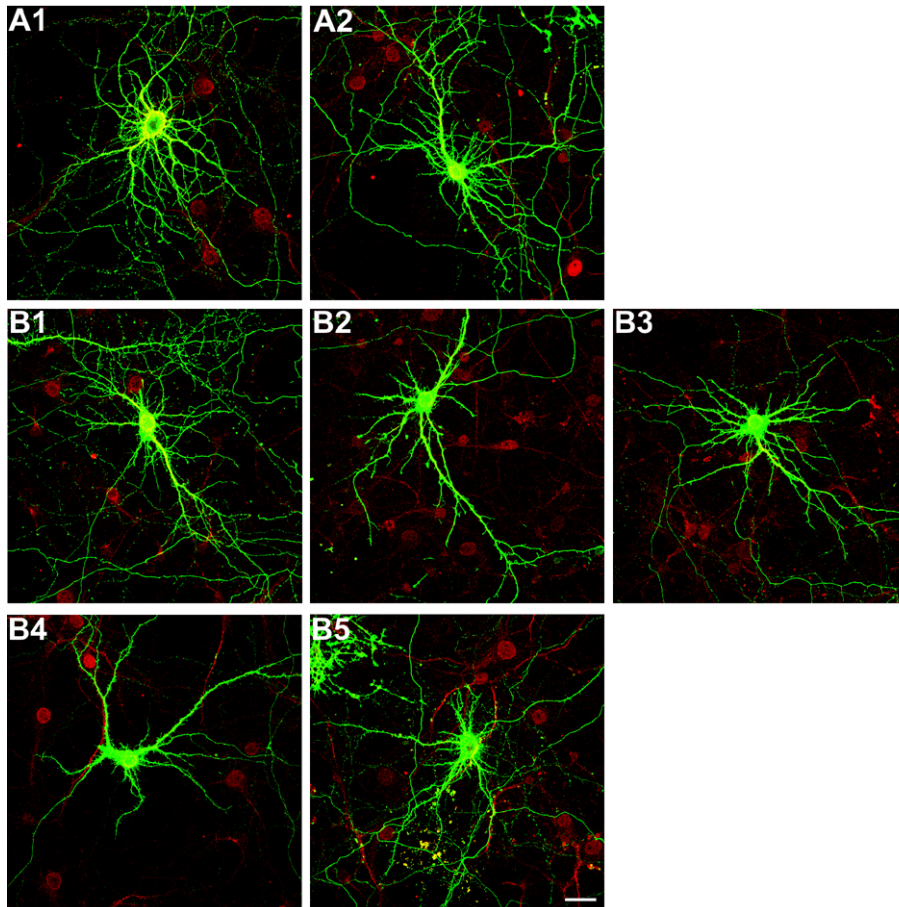
We thank Eva-Maria Stübe and Monika Dulinski for excellent technical, and Kimberly Mason for excellent editorial assistance. This study was supported by the DFG (grants SFB 665-A2 to RN and SS and 665-B3 to RN).

References

- Aono S, Keino H, Ono T, Yasuda Y, Tokita Y, Matsui F, Taniguchi M, Sonta S, Oohira A (2000) Genomic organization and expression pattern of mouse Neuroglycan C in the cerebellar development. *J Biol Chem* **275**: 337–342
- Atwal JK, Massie B, Miller FD, Kaplan DR (2000) The TrkB-Shc site signals neuronal survival and local axon growth via MEK and PI3-kinase. *Neuron* **27**: 265–277
- Banker G, Goslin K (eds). (1998) *Culturing Nerve Cells*. Cambridge, MA: MIT Press
- Brewer GJ, Torricelli JR, Evege EK, Price PJ (1993) Optimized survival of hippocampal neurons in B27-supplemented neurobasal, a new serumfree medium combination. *J Neurosci Res* **35**: 567–576
- Brummelkamp TR, Bernards R, Agami R (2002) A system for stable expression of short interfering RNAs in mammalian cells. *Science* **296**: 550–553
- Chen JG, Rašin MR, Kwan KY, Šestan N (2005) Zfp312 is required for subcortical axonal projections and dendritic morphology of deep-layer pyramidal neurons of the cerebral cortex. *Proc Natl Acad Sci USA* **102**: 17792–17797
- Deuel TAS, Liu JS, Corbo JC, Yoo SY, Rorke-Adams LB, Walsh CA (2006) Genetic interactions between doublecortin and doublecortin-like kinase in neuronal migration and axon outgrowth. *Neuron* **49**: 41–53
- Ethell IM, Pasquale EB (2005) Molecular mechanisms of dendritic spine development and remodeling. *Prog Neurobiol* **75**: 161–205
- Fox IJ, Kornblum HI (2005) Developmental Profile of erbB receptors in murine central nervous system: implications for functional interactions. *J Neurosci Res* **79**: 584–597
- Govek EE, Newey SE, Akerman CJ, Cross JR, Van der Veken L, Van Aelst L (2004) The X-linked mental retardation protein oligophrenin-1 is required for dendritic spine morphogenesis. *Nat Neurosci* **7**: 364–372
- Govek EE, Newey SE, Van Aelst L (2005) The role of Rho GTPases in neuronal development. *Genes Dev* **19**: 1–49
- Hassel B, Schreff M, Stübe EM, Blaich U, Schumacher S (2003) CALEB/NGC interacts with the Golgi-associated protein PIST. *J Biol Chem* **278**: 40136–40143
- Hering H, Sheng M (2001) Dendritic spines: structure, dynamics and regulation. *Nat Rev Neurosci* **2**: 880–888
- Horch HW, Katz LC (2002) BDNF release from single cells elicits local dendritic growth in nearby neurons. *Nat Neurosci* **5**: 1177–1184
- Hou L, Klann E (2004) Activation of the phosphoinositide 3-kinase-Akt-mammalian target of rapamycin signaling pathway is required for metabotropic glutamate receptor-dependent long-term depression. *J Neurosci* **24**: 6352–6361
- Jan YN, Jan LY (2003) The control of dendrite development. *Neuron* **40**: 229–242
- Jaworski J, Spangler S, Seeburg DP, Hoogenraad CC, Sheng M (2005) Control of dendritic arborization by the phosphoinositide-3'-kinase-Akt-mammalian target of rapamycin pathway. *J Neurosci* **25**: 11300–11312
- Ji Y, Pang PT, Feng L, Lu B (2005) Cyclic AMP controls BDNF-induced TrkB phosphorylation and dendritic spine formation in mature hippocampal neurons. *Nat Neurosci* **8**: 164–172
- Jüttner R, Moré MI, Das D, Babich A, Meier J, Henning M, Erdmann B, Müller EC, Otto A, Grantyn R, Rathjen FG (2005) Impaired synapse function during postnatal development in the absence of CALEB, an EGF-like protein processed by neuronal activity. *Neuron* **46**: 233–245
- Kinugasa Y, Ishiquro H, Tokita Y, Oohira A, Ohmoto H, Higashiyama S (2004) Neuroglycan C, a novel member of the neuregulin family. *Biochem Biophys Res Commun* **321**: 1045–1049
- Koizumi H, Tanaka T, Gleeson JG (2006) *Doublecortin-like kinase* functions with *doublecortin* to mediate fiber tract decussation and neuronal migration. *Neuron* **49**: 55–66
- Kumar V, Zhang MX, Swank MW, Kunz J, Wu GY (2005) Regulation of dendritic morphogenesis by Ras-PI3K-Akt-mTOR and Ras-MAPK signaling pathways. *J Neurosci* **25**: 11288–11299
- Kuruvilla R, Ye H, Ginty DD (2000) Spatially and functionally distinct roles of the PI3-K effector pathway during NGF signaling in sympathetic neurons. *Neuron* **27**: 499–512
- Leemhuis J, Boutillier S, Barth H, Feuerstein TJ, Brock C, Nurnberg B, Aktories K, Meyer DK (2004) Rho GTPases and

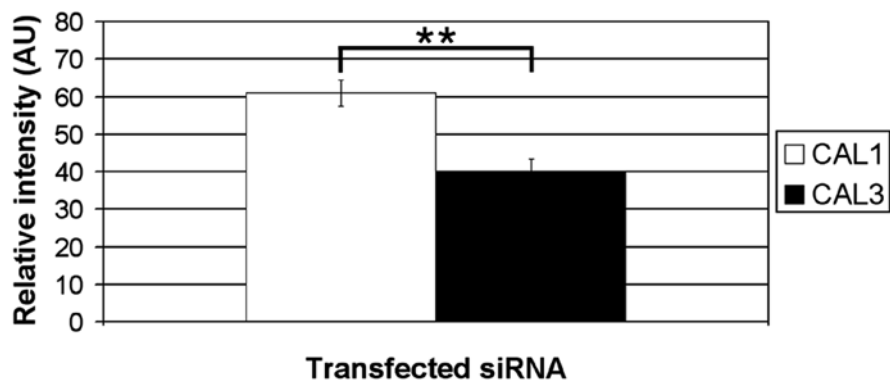
- phosphoinositide 3-kinase organize formation of branched dendrites. *J Biol Chem* **279**: 585–596
- Maletic-Savatic M, Malinow R, Svoboda K (1999) Rapid dendritic morphogenesis in CA1 hippocampal dendrites induced by synaptic activity. *Science* **283**: 1923–1927
- Markus A, Zhong J, Snider WD (2002) Raf and akt mediate distinct aspects of sensory axon growth. *Neuron* **35**: 65–76
- McAllister AK, Katz LC, Lo DC (1996) Neurotrophin regulation of cortical dendritic growth requires activity. *Neuron* **17**: 1057–1064
- Nakanishi K, Aono S, Hirano K, Kuroda Y, Ida M, Tokita Y, Matsui F, Oohira A (2006) Identification of neurite outgrowth-promoting domains of neuroglycan C, a brain-specific chondroitin sulfate proteoglycan, and involvement of phosphatidylinositide 3-kinase and protein kinase C signaling pathways in neuritogenesis. *J Biol Chem* **281**: 24970–24978
- Portera-Cailliau C, Pan DT, Yuste R (2003) Activity-regulated dynamic behavior of early dendritic protrusions: evidence for different types of dendritic filopodia. *J Neurosci* **23**: 7129–7142
- Redmond L, Oh SR, Hicks C, Weinmaster G, Ghosh A (2000) Nuclear Notch 1 signaling and the regulation of dendritic development. *Nat Neurosci* **3**: 30–40
- Saito T, Nakatsuji N (2001) Efficient gene transfer into the embryonic mouse brain using *in vivo* electroporation. *Dev Biol* **240**: 237–246
- Sanna PP, Cammalleri M, Berton F, Simpson C, Lutjens R, Bloom FE, Francesconi W (2002) Phosphatidylinositide 3-kinase is required for the expression but not for the induction or the maintenance of long-term potentiation in the hippocampal CA1 region. *J Neurosci* **22**: 3359–3365
- Schumacher S, Jung M, Nörenberg U, Dorner A, Chiquet-Ehrismann R, Stuermer CAO, Rathjen FG (2001) CALEB binds via its acidic stretch to the fibrinogen-like domain of tenascin-C or tenascin-R and its expression is dynamically regulated after optic nerve lesion. *J Biol Chem* **276**: 7337–7345
- Schumacher S, Stübe EM (2003) Regulated binding of the fibrinogen-like domains of tenascin-R and tenascin-C to the neural EGF family member CALEB. *J Neurochem* **87**: 1213–1223
- Schumacher S, Volkmer H, Buck F, Otto A, Tárnok A, Roth S, Rathjen FG (1997) Chicken acidic leucine-rich EGF-like domain containing brain protein (CALEB), a neural member of the EGF family of differentiation factors, is implicated in neurite formation. *J Cell Biol* **136**: 895–906
- Scott EK, Luo L (2001) How do dendrites take their shape? *Nat Neurosci* **4**: 359–365
- Šestan N, Artavanis-Tsakonas S, Rakic P (1999) Contact-dependent inhibition of cortical neurite growth mediated by Notch signaling. *Science* **286**: 741–746
- Shi SH, Cheng T, Jan LY, Jan YN (2004a) The immunoglobulin family member dendrite arborization and synapse maturation 1 (Dasm1) controls excitatory synapse maturation. *Proc Natl Acad Sci USA* **101**: 13346–13351
- Shi SH, Cox DN, Wang D, Jan LY, Jan YN (2004b) Control of dendrite arborization by an Ig family member, dendrite arborization and synapse maturation 1 (Dasm1). *Proc Natl Acad Sci* **101**: 13341–13345
- Sholl DA (1953) Dendritic organization in the neurons of the visual and motor cortices of the cat. *J Anat* **87**: 387–406
- Sin WC, Haas K, Ruthazer ES, Cline HT (2002) Dendrite growth increased by visual activity requires NMDA receptor and Rho GTPases. *Nature* **419**: 475–480
- Tang SJ, Reis G, Kang H, Gingras AC, Sonenberg N, Schuman EM (2002) A rapamycin-sensitive signaling pathway contributes to long-term synaptic plasticity in the hippocampus. *Proc Natl Acad Sci USA* **99**: 467–472
- Tolias KF, Bikoff JB, Burette A, Paradis S, Harrar D, Tavazoie S, Weinberg RJ, Greenberg ME (2005) The Rac1-GEF Tiam1 couples the NMDA receptor to the activity-dependent development of dendritic arbors and spines. *Neuron* **45**: 525–538
- Vaillant AR, Zanassi P, Walsh GS, Aumont A, Alonso A, Miller FD (2002) Signaling mechanisms underlying reversible, activity-dependent dendrite formation. *Neuron* **34**: 985–998
- Whitford KL, Dijkhuizen P, Polleux F, Ghosh A (2002) Molecular control of cortical dendrite development. *Annu Rev Neurosci* **25**: 127–149
- Wu GY, Deisseroth K, Tsien RW (2001) Spaced stimuli stabilize MAPK pathway activation and its effects on dendritic morphology. *Nat Neurosci* **4**: 151–158
- Yacoubian TA, Lo DC (2000) Truncated and full-length TrkB receptors regulate distinct modes of dendritic growth. *Nat Neurosci* **3**: 342–349
- Yu X, Malenka RC (2003) β -catenin is critical for dendritic morphogenesis. *Nat Neurosci* **6**: 1169–1177
- Yuste R, Bonhoeffer T (2004) Genesis of dendritic spines: insights from ultrastructural and imaging studies. *Nat Rev Neurosci* **5**: 24–34

Supplementary Figure 1 Overlays of micrographs shown in figure 2A and 2B. Scale bar, 20 μm .

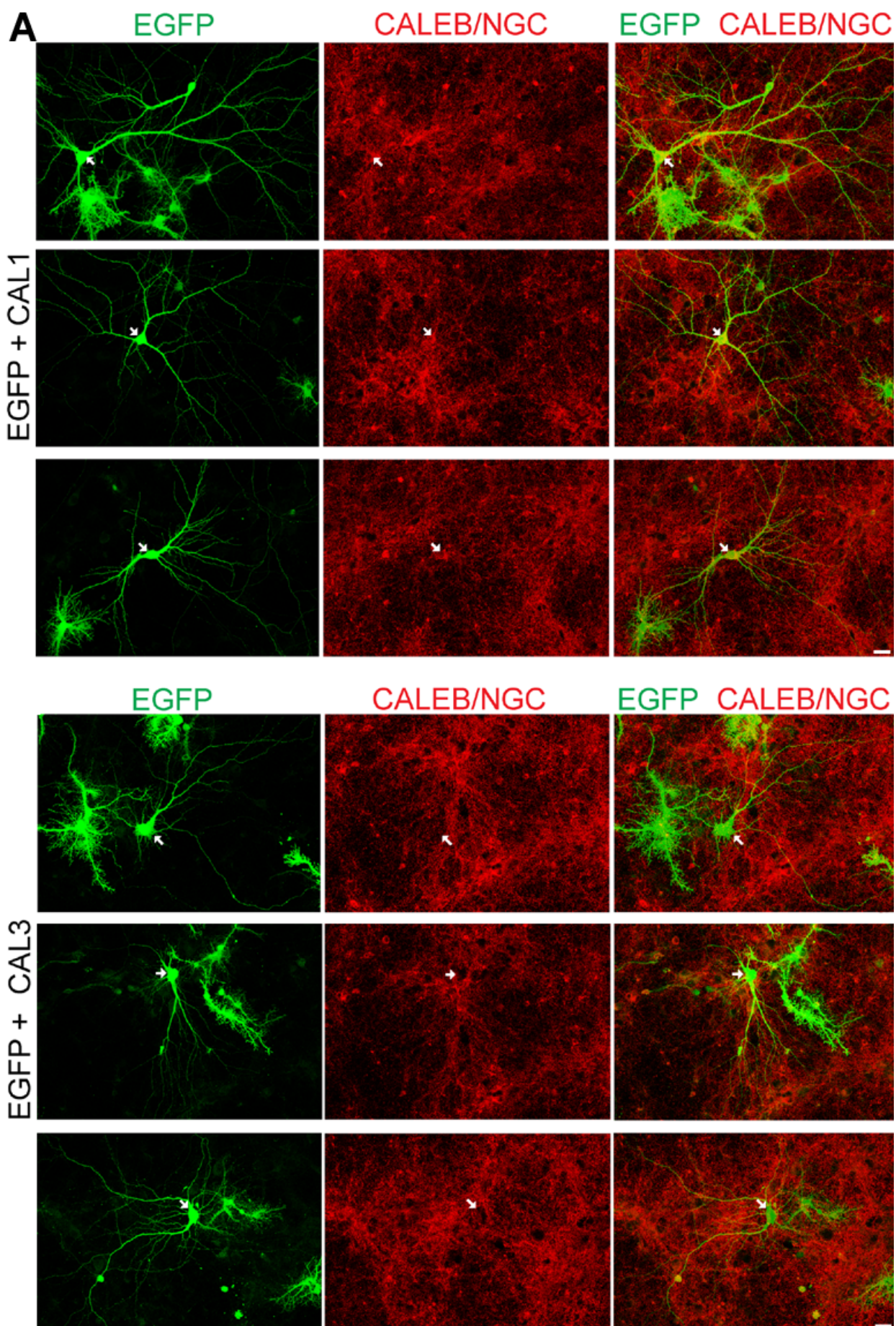


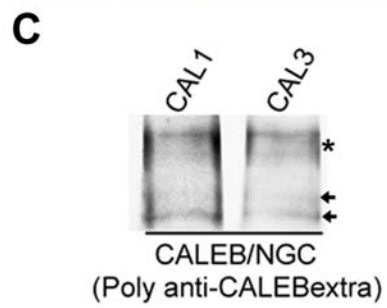
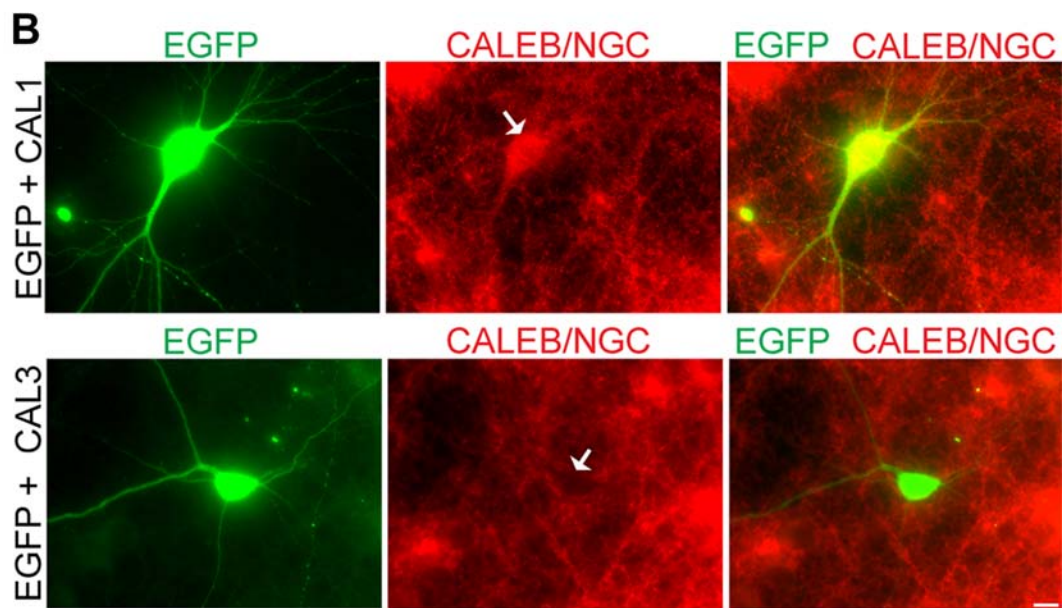
Supplementary Figure 2 RNAi knockdown of endogenous CALEB/NGC expression in hippocampal neurons. DIV10 hippocampal neurons in culture were transfected either with control siRNA CAL1 or with siRNA CAL3 which is specific for CALEB/NGC. Two days after transfection detergent extracts (TBS with 1.2 % TX100 supplemented with protease inhibitors aprotinin, leupeptin, pepstatin and PMSF) of these transfected cells were prepared, separated with SDS-PAGE, and a Western blot was performed with a monoclonal antibody to CALEB/NGC (BD Biosciences). After Western blotting protein bands exposed on X-ray films (Hyperfilm ECL, Amersham Biosciences) were scanned and analyzed using Alpha Ease FC Software (Alpha Imager; Alpha Innotech Corporation; Version 4 1.0; San Leandro, CA 94577, USA).

A quantification of Western blots from three independent experiments is shown ($n = 3$; 40 ± 3.4 for CAL3, and 61 ± 3.4 for CAL1, $**p < 0.01$).



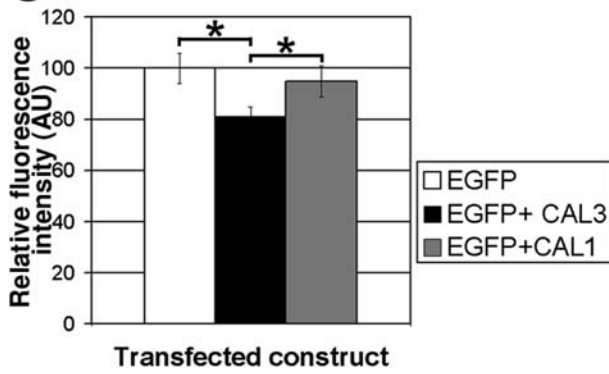
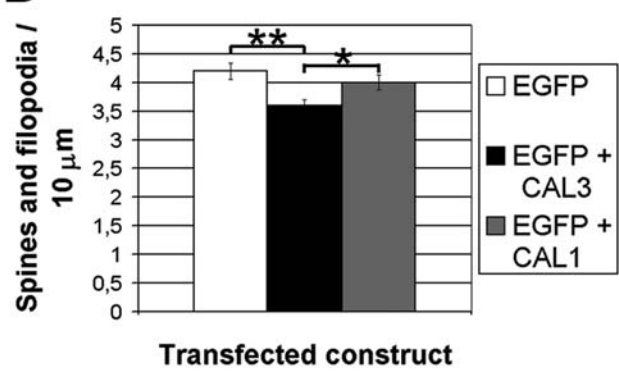
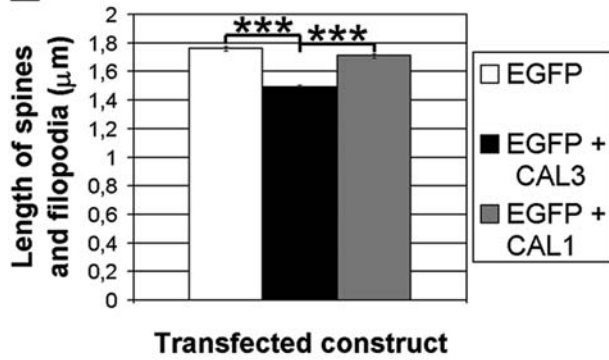
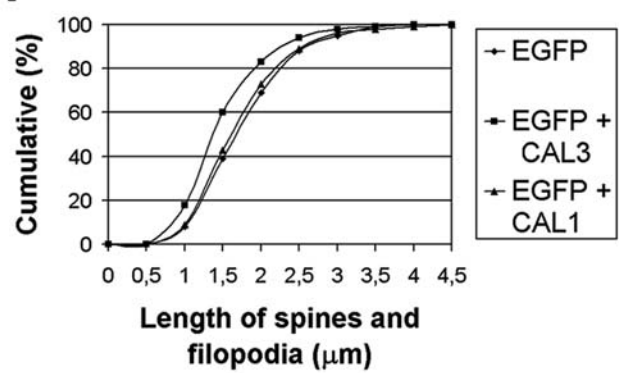
Supplementary Figure 3 Reduction of endogenous CALEB/NGC expression in hippocampal neurons via siRNA results in a decrease in total dendritic end tip number. **(A)** Hippocampal neurons co-transfected at DIV10 with EGFP-encoding plasmid and either CALEB/NGC-specific siRNA CAL3 or CAL1 control siRNA (materials and methods) and analyzed at DIV10+2 are shown (left panels, arrows). The endogenous CALEB/NGC expression of the transfected neurons was downregulated by siRNA as demonstrated by staining of the cultures with an affinity-purified polyclonal antibody to the extracellular part of CALEB/NGC (middle panels, arrows). Note the shedding of the aminoterminal part of the extracellular domain of CALEB/NGC (Jüttner *et al*, 2005). Due to this shedding the polyclonal antibody to CALEB/NGC recognized the part of the extracellular domain of CALEB/NGC which is cleaved-off and deposited in the extracellular space. Overlay of both stainings (right panels). Some glial cells can be observed in the cultures which were also transfected with EGFP. **(B)** Micrographs of neurons co-transfected at DIV10 with EGFP and either CAL3 siRNA or CAL1 control siRNA, and analyzed at DIV10+2. Neurons were stained for GFP and for CALEB/NGC with the affinity-purified polyclonal antibody to the extracellular part of CALEB/NGC. Acquisition of images were performed with wide-field epifluorescence. **(C)** Western blot of endogenous CALEB/NGC levels in primary hippocampal neurons transfected at DIV10 with control siRNA CAL1 or CALEB/NGC-specific siRNA CAL3 and analyzed 2 days later. The immunoblot was probed with affinity-purified polyclonal antibody to the extracellular part of CALEB. Both the CALEB/NGC band (*doublet, arrow*) and the proteoglycan variant of CALEB/NGC (*asterisk*) were stained. Scale bars, 12 μ m.





Supplementary Figure 4 Knockdown of endogenous CALEB/NGC levels using siRNA reduces filopodia and spine density and length. **(A,B)** To assess the significance of endogenous CALEB/NGC for spinogenesis, we co-transfected DIV12 hippocampal neurons in culture with EGFP-encoding plasmid and either the CALEB/NGC-specific siRNA oligonucleotide CAL3 (B) or the control oligonucleotide CAL1 (A), and stained cells for GFP two days after transfection. We found in neurons co-transfected with EGFP-encoding plasmid and CAL3 siRNA a smaller number of filopodia and spines, which are shorter (B) when compared to neurons co-transfected with EGFP and CAL1 (A) or EGFP alone (not shown). **(C)** Quantification of the immunofluorescence signals on neuronal cell bodies with an anti-CALEB/NGC antibody (affinity-purified polyclonal antibody to the extracellular part of CALEB/NGC) two days after transfection yielded a similar reduction of CALEB/NGC levels in CAL3-treated, but not CAL1-treated neurons compared to the EGFP control (30 cell bodies counted, * $p < 0.05$) as shown above (Figure 2F). **(D)** The quantification confirmed that knockdown of CALEB/NGC expression by CAL3 siRNA results in a reduced density (number per 10 μm) of filopodia and spines (3.6 ± 0.1 for EGFP + CAL3, 4.2 ± 0.1 for EGFP, 4.0 ± 0.1 for EGFP + CAL1); > 25 neurons examined for each construct, ** $p < 0.001$ and * $p < 0.01$). **(E)** A decrease in CALEB/NGC levels also led to a reduced length of filopodia and spines ($1.5 \pm 0.02 \mu\text{m}$ for EGFP + CAL3, $1.8 \pm 0.02 \mu\text{m}$ for EGFP, $1.7 \pm 0.02 \mu\text{m}$ for EGFP + CAL1; > 1500 filopodia and spines $\leq 4.5 \mu\text{m}$ of > 24 neurons examined for each condition, *** $p < 0.0001$). **(F)** Cumulative frequency plot of filopodia and spine length in neurons transfected and analyzed as in (E).

The outcome of these knockdown experiments is that endogenous CALEB/NGC contributes to both number and morphogenesis of dendritic filopodia and spines. Scale bar, 2.5 μm .

A EGFP + CAL1**B** EGFP + CAL3**C****D****E****F**

Supplementary Figure 5 In utero electroporation, image acquisition and data analysis.

(A) In utero electroporation. In utero electroporation (IUE) experiments were carried out with CD1 or C57BL/6 mice in accordance with a protocol approved by the Committee on Animal Research at Yale University. The morning of a detectable vaginal plug and the first neonatal day were considered to be embryonic day 0.5 (E0.5) and postnatal day 0 (P0), respectively. Plasmids were prepared using EndoFree Plasmid Kit (Qiagen, Hilden, Germany). Pregnant mice were anesthetized at E14.5/15.5. We used E14.5 for electroporation of animals that were analyzed at P14 for spine and filopodia analysis, because it was shown that the survival rate for older animals is slightly better than for animals electroporated at E15.5 (because less time is available to recover from operation before delivering). Otherwise we used P15.5 because the probability to electroporate neurons not migrating to layer II or III is slightly lower. The uterine horns were exposed and two of the pups were randomly chosen for injecting plasmids. 1-2 μ l of DNA solution (4 μ g/ μ l, supplemented with Fast Green) was injected through the uterine wall into the lateral ventricle of the embryo using a pulled glass capillary (World Precision Instruments). Electric pulses were delivered to embryos through the uterine wall with a CUY21 EDIT (Nepagene) or a ECM830 (BTX) square wave electroporator and a pair of platinum electrodes (CUY650P5) (five 50-ms pulses of 40 V with 950-ms intervals) (Saito and Nakatsuji, 2001). The uterine horns were repositioned in the abdominal cavity, and the abdominal wall and skin were sewed up with surgical sutures. 3-8 animals were electroporated for each condition and the electroporated animals were sacrificed at P7 and P14 for analysis.

Due to the chosen time points (E14.5 and E15.5) for electroporation and the position of electrodes during electroporation we could target layer II and III almost only cortical pyramidal neurons but not deeper layer neurons of the cortex, because these neurons are on their migratory pathway or even finished their migration at E14.5 to E15.5 (Donovan *et al*, 2005; LoTurco and Bai, 2006). Interneurons were only occasionally targeted because these

cells do not migrate from the ventricular/subventricular zone to upper layers but migrate from the medial and lateral ganglionic eminence into the cortex (and could thus not be targeted by IUE at the chosen time points, Metin *et al*, 2006). Only very few interneurons choose a migration pattern that includes ventricular/subventricular zone. Furthermore we were able to discriminate the two major neuronal cell types in cortical layer II and III, the pyramidal neurons and the stellate neurons, by cell morphology and orientation of the axon. With all these criteria we were able to select cortical pyramidal neurons of layer II and III for dendritic tree and spine analysis.

References

Donovan SL, Dyer MA (2005) Regulation of proliferation during central nervous system development. *Semin Cell Dev Biol* **16(3)**: 407-21

LoTurco JJ, Bai J (2006) The multipolar stage and disruptions in neuronal migration. *Trends Neurosci* **29(7)**: 407-13

Metin C, Baudoin JP, Rakic S, Parnavelas JG (2006) Cell and molecular mechanisms involved in the migration of cortical interneurons. *Eur J Neurosci* **23(4)**: 894-900

(B) Image acquisition and data analysis. Hippocampal neurons in culture were transfected and fixed at the indicated time points. EGFP-transfected cells were stained with a polyclonal antibody to GFP (ab6556, Abcam), cultures transfected with CALEB/NGC-derived constructs were stained with a monoclonal antibody to the FLAG tag (M2, Sigma). For knockdown experiments, hippocampal neurons were transfected with shRNA or co-transfected with EGFP-encoding plasmid and siRNA. Cells were co-stained with a monoclonal anti-GFP antibody (B-2, Santa Cruz) and a polyclonal antibody to the extracellular part of CALEB/NGC or with a polyclonal antibody to GFP (ab6556, Abcam) and a monoclonal

antibody to CALEB/NGC (Abnova, Mab anti CSPG5, # H00010675-M01). Alexa Fluor 488-conjugated and Cy3-conjugated secondary antibodies were used.

When quantifying the intensity of the immunofluorescence signal in cell bodies of EGFP-expressing neurons in knockdown experiments, the same acquisition settings for each set of control and experimental samples were used. All the imaging was done in the same session for controls and shRNA or siRNA experiments. Acquisition and data analysis were performed by investigators blind to the experimental conditions. Data acquisition for siRNA experiments was done with wide-field epifluorescence using the equipment described above and Metamorph image analysis software (Universal Imaging Corporation). Data acquisition for shRNA experiments was done with a Leica TCS SL scanning confocal microscope with a 40X HCX PL APO, 1.25 NA objective, zoom 1.6, resolution 1024x1024, and line average 4. Pictures for all neurons were composed of 3 μm thick z -stacks with a step-size of 0.5 μm .

All other images were captured on a Leica TCS SP2 or SL scanning confocal microscope with 40X HCX PL APO, 1.25 NA, 63X HCX PL APO, 1.4 NA or 100X PLAN APO, 1.4 NA oil immersion objectives. For dendritic tree and spine analysis, z -stacks were collected at 0.7- μm and 0.2- μm intervals, respectively. For quantification of TNDET in pyramidal neurons from slices of animals treated by *in utero* electroporation, 15- μm -thick z -stacks of confocal images of dendritic trees of electroporated neurons collected at 1- μm intervals were analyzed. All morphometric measurements were done with Metamorph image analysis software, and acquisition and data analysis were performed by investigators blind to the experimental conditions. Dendritic trees of all healthy transfected neurons with more than 5 dendritic end tips were analyzed. All end tips of dendrites longer than 8 μm were counted. Total number of dendritic end tips were determined by morphology and MAP2 stainings. However, MAP2 staining did not label all small dendritic branches. We used immunohistochemistry against GFP to clearly stain all dendritic branches, because in some cases autofluorescence of GFP is too weak to detect all dendritic branches. Axons could be excluded because of their length,

their caliber, and their branching pattern. Side branches leave the axon almost always in a right angle. This is different to dendritic branches. We performed Sholl analysis in the same manner. We counted the intersections manually, because of problems with axon discrimination when using a software. When examining the length of dendritic spines and filopodia, protrusion length was measured from the protrusion's tip to the point where it meets the dendritic shaft. All protrusions between 0.5 μm and 4.5 μm in length were counted.

figure	measured	number of independent experiments	construct	construct	construct	construct	construct	construct
			mean \pm SEM	mean \pm SEM	mean \pm SEM	mean \pm SEM	mean \pm SEM	mean \pm SEM
1C	TNET	5	EGFP	mCALEBb				
			40.1 \pm 1.2	52.7 \pm 1.5				
3C	TNET	3	EGFP	mCALEBb				
			44.0 \pm 2.1	52.4 \pm 2.2				
1F	NDET basal dendrites	2	EGFP	mCALEBb				
			18.5 \pm 1.1	20.7 \pm 1.0				
1F	NDET apical dendrites	2	EGFP	mCALEBb				
			23.7 \pm 1	29.6 \pm 1.4				
1G	NHOD 1st order	2	EGFP	mCALEBb				
			0.2 \pm 0.4	8.8 \pm 0.4				
1G	NHOD 2nd order	2	EGFP	mCALEBb				
			22.7 \pm 1.1	27.2 \pm 1.5				
1G	NHOD 3rd order	2	EGFP	mCALEBb				
			9.6 \pm 0.7	12.4 \pm 0.9				
1G	4th order	2	EGFP	mCALEBb				
			0.7 \pm 0.2	1.4 \pm 0.3				
2C	TNET	3	pCGLH	CAL3sh	CAL1sh			
			29.7 \pm 1.4	19.4 \pm 0.9	28.7 \pm 1.5			
2F	RFI (AU)	4	EGFP	EGFP+CAL3	EGFP+CAL1			
			100 \pm 4.4	86 \pm 4.3	105 \pm 4.6			
2G	TNET	4	EGFP	EGFP+CAL3	EGFP+CAL1			
			29.8 \pm 1.4	26.3 \pm 1.1	29.8 \pm 1.2			
3B	TNET	3	EGFP	mCALEBb	"388"	"400"		
			45.9 \pm 2.1	60.8 \pm 2.6	48.0 \pm 2.2	56.8 \pm 2.4		
3C	TNET	3	EGFP	EGFP+mCALEBb	EGFP"388"	EGFP+"400"		
			44.0 \pm 2.1	52.4 \pm 2.2	46.7 \pm 2.3	51.9 \pm 1.9		
3E	TNET	4	EGFP	EGFP+"396"				
			36.8 \pm 1.5	29.8 \pm 1.2				
3G	TNET	3	EGFP	EGFP+mCALEBb	EGFP+EGFmutant1	EGFP+EGFshedding1		
			33.7 \pm ?	41.1 \pm 1.6	34.5 \pm 1.2	42.8 \pm 2.1		

4G	TNET	3	pCLEG	mCALEBb	"396"	CAL1sh	CAL3sh	
			12.6 ± 0.6	15.7 ± 0.7	10.4 ± 0.6	11.6 ± 0.4	9.3 ± 0.5	
5B	TNET	3	EGFP	mCALEBb	EGFP+LY294002	mCALEBb+LY294002		
			39.2 ± 0.8	45.4 ± 0.9	30.6 ± 0.7	31.5 ± 1.0		
5C	TNET	2	EGFP	mCALEBb	EGFP+Aktinh. I	mCALEBb+Aktinh. I	EGFP+Aktinh. III	mCALEBb+Aktinh. III
			35.3 ± 0.8	43.5 ± 1.0	31.5 ± 0.7	34.2 ± 1.0	27.9 ± 1.1	29.9 ± 1.1
5D	TNET	2	EGFP	mCALEBb	EGFP+R (10 nM)	mCALEBb+R (10 nM)	EGFP+R (100 nM)	mCALEBb+R (100 nM)
			34.9 ± 0.7	43.0 ± 0.9	33.5 ± 0.6	36.2 ± 0.7	32.8 ± 1.0	36.4 ± 1.1
5E	TNET	3	EGFP	mCALEBb	EGFP+U0126	mCALEBb+U0126		
			38.4 ± 0.8	45.4 ± 1.1	39.4 ± 0.8	44.4 ± 1.1		
6B	TNET	4	EGFP	mCALEBb	EGFP+NF/APV/TTX	mCALEBb+NF/APV/TTX		
			36.4 ± 0.9	49.1 ± 0.9	29.8 ± 1.0	38.1 ± 1.9		
6C	TNET	3	EGFP	mCALEBb	EGFP+Hypericin	mCALEBb+Hypericin		
			39.5 ± 0.8	44.7 ± 1.1	39.1 ± 0.8	42.4 ± 1.2		
6D	TNET	2	EGFP	mCALEBb	EGFP+BIM (1 µM)	mCALEBb+BIM (1 µM)	EGFP+BIM (10 µM)	mCALEBb+BIM (10 µM)
			38.3 ± 0.9	45.5 ± 1.2	37.0 ± 1.4	40.5 ± 1.4	38.2 ± 1.5	39.9 ± 1.7
7D	length (µm)	7	EGFP	mCALEBb				
			1.4 ± 0.02	1.6 ± 0.02				
7E	density /10 µm	7	EGFP	mCALEBb				
			3.7 ± 0.11	5.0 ± 0.17				
7F	branchpoints/100 µm	7	EGFP	mCALEBb				
			1.7 ± 0.2	11.8 ± 0.5				
8B	length (µm)	3	EGFP	mCALEBb	"396"	CAL1sh	CAL3sh	
			0.87 ± 0.02	1.06 ± 0.02	0.76 ± 0.02	0.85 ± 0.02	0.76 ± 0.02	
8C	density /10 µm	3	EGFP	mCALEBb	"396"	CAL1sh	CAL3sh	
			6.8 ± 0.3	8.7 ± 0.4	5.6 ± 0.3	7.5 ± 0.3	5.5 ± 0.4	
8D	branchpoints/100 µm	3	EGFP	mCALEBb	"396"	CAL1sh	CAL3sh	
			5.2 ± 1.1	12.0 ± 1.6	2.2 ± 0.6	5.1 ± 0.8	2.8 ± 0.6	
9B	length (µm)	2	EGFP	EGFP+mCALEBb	EGFP+EGFmutant1	EGFP+EGFshedding1		
			1.17 ± 0.02	1.4 ± 0.03	1.19 ± 0.02	1.37 ± 0.02		
9C	density /10 µm	2	EGFP	EGFP+mCALEBb	EGFP+EGFmutant1	EGFP+EGFshedding1		
			5.0 ± 0.02	7.1 ± 0.2	5.3 ± 0.02	6.6 ± 0.2		

9D	branchpoints/100 μm	2	EGFP	EGFP+mCALEBb	EGFP+EGFmutant1	EGFP+EGFshedding1		
			6.0 ± 0.8	12.6 ± 1.0	7.8 ± 0.6	10.8 ± 1.0		
9F	length (μm)	2	EGFP	EGFP+mCALEBb	EGFP+LY294002	EGFP+mCALEBb+LY294002		
			1.34 ± 0.02	1.44 ± 0.02	1.34 ± 0.02	1.42 ± 0.02		
9G	length (μm)	3	EGFP	mCALEBb	EGFP+LY294002	mCALEBb+LY294002		
			1.33 ± 0.01	1.57 ± 0.01	1.35 ± 0.01	1.52 ± 0.01		
9I	length (μm)	2	EGFP	EGFP+mCALEBb	EGFP+Hypericin	EGFP+mCALEBb+Hypericin		
			1.3 ± 0.02	1.46 ± 0.02	1.3 ± 0.02	1.24 ± 0.02		
S4D	density /10 μm	2	EGFP	EGFP+CAL3	EGFP+CAL1			
			4.2 ± 0.1	3.6 ± 0.1	4.0 ± 0.1			
S4E	length (μm)	3	EGFP	EGFP+CAL3	EGFP+CAL1			
			1.8 ± 0.02	1.5 ± 0.02	1.7 ± 0.02			

Supplementary Figure 6 Summary of statistical results

TNDET: total number of dendritic end tips

NHOD: number of higher-order dendrites

RFI: relative fluorescence intensity

AU: arbitrary units